

Three DNA polymerases, recruited by different mechanisms, carry out NER repair synthesis in human cells

Article (Accepted Version)

Ogi, Tomoo, Limsirichaikul, Siripan, Overmeer, René M, Volker, Marcel, Takenaka, Katsuya, Cloney, Ross, Nakazawa, Yuka, Niimi, Atsuko, Miki, Yoshio, Japers, Nicolaas G, Mullenders., Leon H F, Yamashita, Shunichi, Foustieri, Maria I and Lehmann, Alan R (2010) Three DNA polymerases, recruited by different mechanisms, carry out NER repair synthesis in human cells. *Molecular Cell*, 37 (5). pp. 714-727. ISSN 1097-2765

This version is available from Sussex Research Online: <http://sro.sussex.ac.uk/id/eprint/2309/>

This document is made available in accordance with publisher policies and may differ from the published version or from the version of record. If you wish to cite this item you are advised to consult the publisher's version. Please see the URL above for details on accessing the published version.

Copyright and reuse:

Sussex Research Online is a digital repository of the research output of the University.

Copyright and all moral rights to the version of the paper presented here belong to the individual author(s) and/or other copyright owners. To the extent reasonable and practicable, the material made available in SRO has been checked for eligibility before being made available.

Copies of full text items generally can be reproduced, displayed or performed and given to third parties in any format or medium for personal research or study, educational, or not-for-profit purposes without prior permission or charge, provided that the authors, title and full bibliographic details are credited, a hyperlink and/or URL is given for the original metadata page and the content is not changed in any way.

Three DNA polymerases, recruited by different mechanisms, carry out NER repair synthesis in human cells.

Tomoo Ogi^{1*}, Siripan Limsirichaikul^{1+,2}, René M Overmeer³⁺, Marcel Volker⁴⁺, Katsuya Takenaka⁵⁺, Ross Cloney⁴⁺, Yuka Nakazawa¹⁺, Atsuko Niimi^{1,4}, Yoshio Miki⁵, Nicolaas G Jaspers⁶, Leon HF Mullenders^{3#}, Shunichi Yamashita^{1#}, Maria I Foustari^{3#} and Alan R Lehmann^{4*}

¹ Department of Molecular Medicine, Atomic Bomb Disease Institute, Graduate School of Biomedical Sciences, Nagasaki University, 1-12-4, Sakamoto, Nagasaki 852-8523, Japan; tel: +81-95-819-7103 fax: +81-95-819-7104

² Department of Biopharmacy, Faculty of Pharmacy, Silpakorn University, Nakhon Pathom, 73000 Thailand

³ Department of Toxicogenetics, Leiden University Medical Center, Einthovenweg 20, 2333ZC Leiden, Netherlands

⁴ Genome Damage and Stability Centre, University of Sussex, Falmer, Brighton BN1 9RQ, United Kingdom; tel: +44-1273-678-120 fax: +44-1273-678-121

⁵ Department of Molecular Genetics, Medical Research Institute, Tokyo Medical and Dental University, 1-5-45, Yushima, Bunkyo-ku, Tokyo 113-8510, Japan

⁶ Department of Genetics, Erasmus University Medical Centre, Erasmus MC, 3000 CA Rotterdam, Netherlands

^{+,#} These authors contributed equally to this work

^{*} To whom correspondence should be addressed. E-mail: togi@nagasaki-u.ac.jp; a.r.lehmann@sussex.ac.uk

RUNNING TITLE

Cooperative roles of DNA polymerases in NER repair synthesis

SUMMARY

Nucleotide excision repair (NER) is the most versatile DNA repair system that deals with the major UV photoproducts in DNA, as well as many other DNA adducts. The early steps of NER are well understood, whereas the later steps of repair synthesis and ligation are not. In particular, which polymerases are definitely involved in repair synthesis and how they are recruited to the damaged sites has not yet been established. We report that, in human fibroblasts, approximately half of the repair synthesis requires both polk and pol δ and both polymerases can be recovered in the same repair complexes. Polk is recruited to repair sites by ubiquitinated PCNA and XRCC1, pol δ by the classical replication factor complex, RFC1-RFC, together with a polymerase accessory factor, p66, and unmodified PCNA. The remaining repair synthesis is dependent on pol ϵ , recruitment of which is dependent on the alternative clamp loader CHTF18-RFC.

INTRODUCTION

Nucleotide excision repair (NER) is the most versatile DNA repair system that deals with both of the major UV photoproducts in DNA, as well as many other DNA adducts (Friedberg et al., 2005b). Most cases of xeroderma pigmentosum (XP), an extremely sunlight-sensitive and cancer-prone hereditary disease, result from a deficiency in one of the genes involved in NER (Andressoo and Hoeijmakers, 2005). The NER pathway can be divided into early and late steps: the molecular mechanism

of the former, which involves sequential actions of XP proteins that recognise, unwind, and incise the damage, has been well characterised from bacteria to humans. However, the latter step, comprising gap-filling repair synthesis, in which DNA replication proteins fill in the ~30 nucleotide gap, and ligation, has not yet been defined in higher eukaryotes (reviewed in (Gillet and Scharer, 2006; Hanawalt and Spivak, 2008)).

Research on the post incision steps of human NER has been carried out mainly with *in vitro* reconstituted systems with recombinant proteins and/or tissue culture cell lysates (Aboussekhra et al., 1995; Araujo et al., 2000; Nishida et al., 1988). In these systems, the proteins that are involved in replicative DNA synthesis (or even bacterial or viral DNA replication proteins) can carry out the NER resynthesis reaction. Based on the findings of these studies, it has been assumed that both of the replicative DNA polymerases, pol δ and pol ϵ , are responsible for repair synthesis *in vivo*, and that the nick sealing is carried out by DNA Ligase I, similar to S-phase DNA replication (See reviews). Since NER is considered a non-mutagenic process, the above model that the gap-filling step is performed by the high-fidelity B-family DNA polymerases has been widely accepted (Wood and Shivji, 1997), despite the lack of definitive evidence to support this hypothesis.

Contrary to these assumptions, however, our groups have recently reported that an error-prone Y-family DNA polymerase, pol κ , is also involved in NER in mouse cells (Ogi and Lehmann, 2006), and that the XRCC1/Ligase III complex, which interacts with pol β and is involved in single-strand break repair (SSBR) and base-excision repair (BER), is largely responsible for the NER nick ligation process in human cells (Moser et al., 2007).

DNA polymerase loading mechanisms in human cells have been extensively investigated with *in vitro* systems (reviewed in (Johnson and O'Donnell, 2005)). During DNA replication, proliferating cell nuclear antigen (PCNA) is loaded by the replication factor C (RFC) clamp loader complex at the double-strand/single-strand DNA template-primer terminus in an ATP-dependent manner (Majka and Burgers, 2004). Subsequent to PCNA loading, the replicative DNA polymerase can access the replication site through an interaction with PCNA. A similar molecular mechanism has been assumed for NER repair synthesis as the gap remaining after damage incision and removal by XP-proteins leaves a free 3'-OH terminus with an intact template, which is structurally similar to the replication elongation intermediate (Gillet and Scharer, 2006). In contrast, translesion synthesis (TLS), the bypass of DNA lesions that block replication by normal replicative DNA polymerases, involves a polymerase switch from the replicative- to a specialised- DNA polymerase (Friedberg et al., 2005a). Ubiquitination of PCNA, which is dependent on the E3 ubiquitin ligase RAD18, facilitates this process (Moldovan et al., 2007). All Y-family polymerases have both PCNA-binding and ubiquitin-binding motifs, so ubiquitination of PCNA increases its affinity for these polymerases, thereby mediating the polymerase switch (Bienko et al., 2005; Kannouche et al., 2004; Plosky et al., 2006; Watanabe et al., 2004).

Clamp loaders are hetero-pentamers comprising four small subunits, RFC2-5, common to all clamp loaders and a large subunit that varies between complexes (Majka and Burgers, 2004). The classical RFC1-5 pentamer loads PCNA onto the DNA during replication. Because of their ability to interact with DNA polymerases,

RFC complexes have been often implicated in loading different DNA polymerases themselves as well as loading PCNA and the alternative sliding clamp, 9-1-1 (Kai and Wang, 2003; Masuda et al., 2007; Shiomi et al., 2007). The polk homolog in *S. pombe*, DinB, is reported to be recruited to the replication fork by the 9-1-1 checkpoint clamp and Rad17 clamp loader complex, when the replication machinery encounters DNA damage (Kai and Wang, 2003).

Here we describe roles of three DNA polymerases, pol δ , pol ϵ and polk, which we show are responsible for human NER repair synthesis *in vivo*. siRNA depletion of these polymerases diminished the repair synthesis activity *in vivo*. Recruitment of these polymerases into NER repair sites are differentially regulated by the status of PCNA ubiquitination as well as by usage of distinct clamp loader complexes or the repair scaffolding protein XRCC1. Based on the above findings, we propose a model for the involvement of mutagenic and conventional DNA polymerases and their differential loading mechanisms in NER repair synthesis.

RESULTS

UV damage induces PCNA ubiquitination in quiescent human cells

In previous work we and many other groups have highlighted the importance of PCNA ubiquitination in the regulation of TLS during replication of damaged DNA (Lehmann et al., 2007). TLS usually employs Y-family DNA polymerases (Ohmori et al., 2001), which are recruited to ubiquitinated PCNA because they have binding motifs for both PCNA (PIP box) and ubiquitin (UBZ motif) (Bienko et al., 2005). We were interested to discover if ubiquitinated PCNA might have functions outside of S phase, so we examined primary human fibroblasts which were maintained for several

days in low serum to bring them into quiescence. Figure 1A shows that UV-irradiation did indeed result in PCNA ubiquitination in normal (48BR) cells (lanes 2-4), albeit at much lower levels than in exponentially growing SV40-transformed MRC5V1 cells (lane 1). Remarkably, a similar induction of PCNA ubiquitination was observed in XP-A (lanes 5-7) and XP-C cells (lanes 8-10), indicating that, although UV-dependent, it was independent of incision during NER. In all cases, the ubiquitinated PCNA was resistant to extraction by Triton-X100, indicating that it was bound to chromatin (Figure 1B).

The number of S-phase cells in these cultures was negligible, as measured by the expression of cycling marker ki67 and nucleoside incorporation (Supplementary Experimental Procedures), so there could be no involvement in replication-associated processes. Furthermore hydroxyurea (HU) treatment for up to 4 hours, which stalls cells in S phase, did not elicit the ubiquitination of PCNA in quiescent normal (Figure 1C, lanes 4,5) or xeroderma pigmentosum (XP) (lanes 8,9 for XP-A, and lanes 12,13 for XP-C) cells, though it did, as shown previously, induce PCNA ubiquitination in cycling populations in S-phase (Figure 1C, lane 2) (Bienko et al., 2005).

Ubiquitinated PCNA is associated with proteins involved in the late step of NER

Although the results of Figure 1A indicate that PCNA ubiquitination was not dependent on damage incision during NER, we were interested to discover if it might nevertheless play a role in later steps of NER. In previous work, we have used chromatin immunoprecipitation (ChIP) to identify protein complexes involved in different stages of NER (Fousteri et al., 2006; Moser et al., 2007). In particular we were able to identify a complex that was UV- dependent and contained proteins

involved in the late, post-incision, steps of NER, including RPA, XRCC1 and PCNA. Figure 1D and 1E show immunoblots revealing some of the components of this complex following ChIP with anti-PCNA antibody from normal cells under various different conditions. Remarkably, a band corresponding to ubiquitinated PCNA was easily observable in these ChIPs. This band was dependent on UV-irradiation and could be observed both in serum-starved (G0) cells (lanes 1,2) and cycling cells close to confluence (lanes 3, 4). This represents a considerable enrichment of the ubiquitinated PCNA relative to unmodified PCNA (compare relative intensities of modified and unmodified bands in Figures 1D, 1E and 1A). We noted in these complexes the presence of pol δ both in G0 cells and in cycling cells (Figure 1D), consistent with our previous observations (Moser et al., 2007), and also pol ϵ only in cycling cells (Figure 1E). Both these DNA polymerases have been previously implicated in NER repair synthesis in an *in vitro* reconstituted system (Araujo et al., 2000). Pol η , which is involved in translesion synthesis of cyclobutane pyrimidine dimers (CPDs), was barely detectable in the ChIP (Figure 1E, lane 4). Importantly, the complex also contained pol κ (Figure 1D), which we have previously shown to be involved in NER in mouse embryonic fibroblasts (Ogi and Lehmann, 2006). The amount of pol κ in the ChIP was significantly higher in G0 cells than in cycling cells (compare lanes 2 and 4). The cellular dNTP levels are reduced in quiescent cells, so this finding supports our previous proposal that pol κ might be the optimal polymerase for NER repair replication when dNTP concentrations are low (Ogi and Lehmann, 2006). Very little of the above proteins were precipitated from unirradiated cells (lanes 1 and 3), confirming that these interactions were DNA damage specific. We did not observe any significant interaction in a similar ChIP with anti-PCNA antibody from NER-deficient non-dividing XPA cells (Figure 1F, lanes 1,2). Importantly, the

same proteins were obtained in the converse experiment using anti-polk (Figure 1G) as well as anti-XRCC1 (Figure 1H) antibodies for the ChIPs. In particular Figure 1G shows that polk and δ are present in the same repair complex.

Recruitment of DNA polymerase κ into repair sites is dependent on NER-damage incision

To determine if ubiquitinated PCNA is required for recruitment of DNA polymerases to NER complexes, we have employed the technique of irradiation of non-dividing primary human fibroblasts through a micropore filter to generate damage in localised parts of the nucleus (Volker et al., 2001). We then analysed the accumulation of polymerases at the sites of local damage (ALD). Using anti-polk antibodies that detect endogenous levels of polk (Figures S1A, S1B), we were able to observe polk ALD following UV-irradiation of confluent primary human fibroblasts, where it colocalised with DNA damage (Figure S2A) and with RPA (Figure 2A). Using *POLK* siRNA, we confirmed that these ALD “spots” did indeed represent polk (Figure 2B, S2B).

Polk ALD could be observed either in quiescent cells, or in cycling cells outside of S phase (Figure S2C), but was not seen in S phase cells (Figure S2D). We previously showed that polk, unlike the other Y-family polymerases, is rarely located in replication factories (Ogi et al., 2005). The intensity of the ALD spots could be amplified by incubation in hydroxyurea after UV-irradiation (Figures S2E, S2F, right panels). We have occasionally used HU in ALD experiments to obtain clearer images, but in all cases, we have observed similar phenomena with and without the inhibitor, any differences being quantitative rather than qualitative.

We next used XP cells from different complementation groups, whose gene products function in the pre-incision and dual incision steps of global NER. In XP-A (Figure 2C), -C, and -G cells, and in cells depleted of XPF (Figures S2G-2I), polk ALD was abolished, whereas it did accumulate at damaged sites in co-cultivated normal cells that were loaded with latex beads to distinguish them from the XP cells. Polk ALD was not affected in Cockayne Syndrome (CS-B) cells, which are defective in the transcription-coupled branch of NER (TCR, which only contributes to ~5% of the entire NER activity) (Figure S2J). These results show that in human primary fibroblasts, polk is involved in a late stage of NER that is dependent on successful completion of the early incision steps.

Role of DNA polymerase κ in NER repair synthesis is dependent on its UBZ Zn-finger domain and PCNA ubiquitination by *RAD18*

We next examined if recruitment of pol κ during NER was dependent on PCNA ubiquitination. A key enzyme required to ubiquitinate PCNA is the E3 ubiquitin ligase RAD18 (Hoege et al., 2002; Kannouche et al., 2004; Watanabe et al., 2004). In a previous report, Rad18 was shown to regulate polk recruitment to stalled replication forks during translesion synthesis of bulky DNA adducts (Bi et al., 2006). We therefore examined the effect of depleting RAD18 on ALD of polk in NER repair synthesis. In these experiments, we cocultivated cells treated with a non-targeting control and loaded with latex beads with cells treated with a specific *RAD18* siRNA. Depletion of RAD18 resulted in a reduction in polk ALD (Figure 3A right panel, compare nuclei indicated with green (polk ALD negative) and white (polk ALD positive) arrows); we also confirmed that PCNA ubiquitination after UVC irradiation

was completely abolished in the cells treated with *RAD18* siRNA (Figure 3B). The ALD data are quantitated in Figure 3C.

Polk contains two C2HC ubiquitin-binding zinc finger (UBZ) motifs that are required for binding of polk to ubiquitinated PCNA (Bienko et al., 2005; Guo et al., 2008). Apart from the cysteine residues, D644 and D799 are crucial aspartate residues that are essential for binding of the zinc finger to ubiquitin (Bienko et al., 2005). We mutated different residues in one or both of these motifs and found that this abolished polk ALD (Figure 3D). (Figure S2K shows that the levels of expression of the different GFP-polk constructs. This varied about twofold between cells expressing different constructs, but there was no correlation between expression level and ALD).

ALD and ChIP measure the recruitment of proteins to the sites of DNA damage but do not prove unequivocally that they are required for repair of the damage. We therefore measured the repair replication step of NER, using a novel fluorescence-based variation of the unscheduled DNA repair synthesis (UDS) assay by incorporation of a thymidine analogue, ethynyl deoxyuridine (Figures S3A , S3B) (Limsirichaikul et al., 2009). As shown in Figures 3E and S3C , depleting cells of polk yielded a substantial reduction in UDS, similar to the reduction that we previously observed in *Polk* deficient mouse embryonic fibroblasts (Ogi and Lehmann, 2006). Depletion of RAD18 resulted in a comparable level of reduction in UDS and depletion of both RAD18 and polk resulted in only a slight further reduction. In order to rule out any off-target effects from these pools of four siRNAs, we also analysed the effects of each siRNA individually. Figure S3D shows that each individual siRNA had a similar effect to the pool, ruling out any off-target effects. Taken together, the data of Figures 1-3 suggest that polk is recruited to sites of NER by binding to

ubiquitinated PCNA, where it is involved in repair synthesis at about 50% of the repair sites.

Pol δ and NER

Mammalian pol δ contains four subunits, p125, p66, p50 and p12 (Podust et al., 2002). p125 and p50 are the catalytic-core subunits (Lee et al., 1991), and p66 is an accessory factor that binds to PCNA (Hughes et al., 1999). Confirming our previous results (Moser et al., 2007), pol δ accumulates at local damage, as shown for both p125 and p66 in Figure 3A (middle panel for p125), and 4A (top panels for p125, and middle panels for p66). In contrast to pol κ , ALD of p125 and p66 were unaffected by depletion of RAD18 (compare green and white arrows in Figure 3A; quantitation in Figure 3C), suggesting that ubiquitination of PCNA is not required for recruitment of pol δ to NER sites following incision by the XP proteins.

We next investigated the interdependency of pol κ and pol δ for relocation to DNA damage. We anticipated that the localisation of pol κ might be dependent on the p66 subunit of pol δ as p66 has been implicated in recruiting translesion polymerases to stalled replication forks in yeast (Gerik et al., 1998; Gibbs et al., 2005). Additionally, the contribution of p66 to recruiting the pol δ catalytic core to PCNA loaded onto DNA is still contentious: Pol32p, the p66 subunit of yeast pol δ , is dispensable for cell viability, suggesting that it is not essential for DNA synthesis itself (Gerik et al., 1998); some *in vitro* evidence also suggests that DNA synthesis activity of pol δ stimulated by PCNA may not be strongly dependent on p66 (Podust et al., 2002; Zhou et al., 1997), although contradictory data have also been reported (Ducoux et al., 2001; Masuda et al., 2007; Shikata et al., 2001). To determine the roles of p66 in NER

repair synthesis, we examined the effects of siRNA depletion of *POLD3* (p66) as well as *POLD1* (p125) on ALD of the polymerases. Interestingly, ALD of pol δ p125 catalytic-core was dependent on the p66 subunit (Figure 4A, top, right panel; Figure 4B), whereas ALD of the p66 subunit was independent of p125 (middle center panel); this observation favors the previous reports suggesting that p66 is crucial for DNA synthesis (Ducoux et al., 2001; Masuda et al., 2007; Shikata et al., 2001). ALD of pol κ was not dependent on either subunit of pol δ (bottom); in fact, depletion of the pol δ subunit(s) resulted in a modest increase in pol κ ALD (Figure 4B). These data show that pol κ and δ are recruited to damage independently and that recruitment of pol δ requires its p66 subunit.

DNA polymerases δ , ϵ , and κ but neither β , η , nor ι are responsible for NER repair synthesis

We next examined the effects of DNA polymerase δ depletion on repair synthesis activity. As shown in Figure 4C (See also Figure [S3C](#)), depleting cells of the p125 (*POLD1*) or p66 (*POLD3*) subunits of pol δ resulted in a 50% reduction in UDS, as observed with pol κ depletion. However depletion of either subunit of pol δ together with pol κ had no further effect, suggesting that these two polymerases play roles in the same sub-pathway of repair replication. This conclusion is supported by the finding of both polymerases in the same repair complex, as shown above in Figure 1G. To determine which polymerase might be responsible for the remaining ~50% of UDS when both pol κ and/or δ are depleted, we examined the effects on UDS of depleting other polymerases. Pol β is well known to interact with the XRCC1/Lig3 complex, which we recently showed was involved in the ligation step of NER (Moser et al., 2007); however, in the same report, we failed to demonstrate the recruitment of

pol β into NER repair sites (Moser et al., 2007). Consistent with this report, we found that depletion of pol β (*POLB*) had no significant effect on UDS, as was also the case for depletion of the Y-family polymerases η or ι (Figure 4D). In striking contrast, depletion of pol ϵ reduced UDS by about 50% (Figure 4D). Depletion of pol ϵ together with pol β did not elicit any further decrease (Figure 4D), but depletion of both pol ϵ and either pol δ (*POLD3*) or pol κ reduced UDS to about 25% and depletion of all three left only 10-15% of the level in normal cells (Figure 4E). Since this is also the level that we observed in cells depletion of *XPA*, or a completely NER-defective XP-A cell strain (Figures 4E, S3C, S3D, and (Limsirichaikul et al., 2009)), we regard this as the detection limit of the technique, and conclude that pol ϵ is indeed responsible for the repair synthesis that is not completed by pol δ and κ . Consistent with this we were able to detect ALD of pol ϵ under mild permeabilisation conditions (Figure S4A). Whereas ALD of all other proteins was resistant to Triton-X 100 extraction, pol ϵ that had accumulated at local damage was extracted by the same triton treatment (Figure S4B). This suggests that pol ϵ is less tightly bound to chromatin than other proteins or that it is bound more transiently. Taken together, our data show that three polymerases pols δ , ϵ , and κ are responsible for almost the entire repair synthesis in primary human cells.

Differential DNA polymerase loading mechanisms in NER repair synthesis

The above findings prompted us to consider differential polymerase recruitment mechanisms in NER repair synthesis, as the recruitment kinetics as well as the epistatic effects of polymerase depletions on UDS seemed different between pol δ/κ and pol ϵ .

We first attempted to find out if any other clamps, clamp loaders and scaffold proteins were required for recruitment of pols δ and κ during NER. We expected that the involvement of (unmodified) PCNA in the recruitment of pol δ and of ubiquitinated PCNA in recruitment of pol κ would implicate a clamp-loading complex in the recruitment of these polymerases. Although depletion of RFC1, RFC4 or both subunits reduced ALD of pol δ -p125, surprisingly it had no effect on ALD of either pol κ or pol δ -p66 (Figure 5A, 5B). This finding indicates that the recruitment of DNA polymerases may not require post-UV loading of PCNA onto chromatin by the conventional RFC1-RFC. Additionally, RFC-independent p66 recruitment is consistent with a recent publication suggesting that p66 can compete with RFC and prevent pre-loaded PCNA being unloaded or relocated from the 3' termini of replication sites by RFC (Masuda et al., 2007).

We next examined the effects of depleting either the checkpoint clamp-loader RAD17 and also the checkpoint activator ATR. We found no significant effect on ALD of pol κ or pol δ (Figure 5A), in contrast to a report that the *S. pombe* ortholog of pol κ is recruited to stalled replication forks by Rad17 and the 9-1-1 complex (Kai and Wang, 2003). Depletion of two other alternative clamp loader large subunits CHTF18, or FRAG1 had no effect on ALD of pol κ , pol δ -p66 or pol δ -p125 (Figure 5A). In contrast, the scaffold protein XRCC1, previously shown to be a component of the post-incision complex (Moser et al., 2007), was needed for ALD of pol κ (Figure 5A, 5C). Depletion of any of the factors needed for ALD of pol δ or pol κ also resulted in a 50% reduction in UDS, whereas depletion of ATR or Rad17 had very little effect on repair synthesis (Figure 5D). In summary these experiments suggest that pol δ -p125 is loaded onto PCNA by RFC1-RFC and p66, whereas pol κ is loaded onto

ubiquitinated PCNA and requires XRCC1 but not RFC. Failure to load either of these polymerases results in a reduction in UDS to about 50% of its normal level, similar to that found by depleting the polymerases.

We have further examined whether any of the loading factors might also be needed for ALD of pol ϵ . As shown in Figure 5E, depletion of RAD18 did not elicit any reduction in pol ϵ ALD, suggesting that pol ϵ is loaded onto unmodified PCNA. Depletion of XRCC1 or the alternative clamp loader large subunits, RAD17 or FRAG1, did not affect pol ϵ ALD; however, depletion of either RFC4, or CHTF18 resulted in a reduction in pol ϵ ALD, suggesting that CHTF18-RFC is involved in loading pol ϵ in repair synthesis (Figures 5E, 5F). CHTF18 is the human homologue of yeast Ctf18p, which is essential for accurate chromosome transmission, being implicated in sister chromatid cohesion (Hanna et al., 2001) and double strand break repair (Ogiwara et al., 2007). Additionally, recent reports demonstrated that CHTF18-RFC can stimulate the activity of pol η (Shiomi et al., 2007) as well as pol δ (Bermudez et al., 2003), suggesting that CHTF18-RFC may play a role in loading specific polymerases during replication when needed.

We also observed a modest reduction of pol ϵ ALD in cells depleted of RFC1 (Figure 5E); however, because of the aforementioned technical issue, the experimental errors were substantially larger than errors in ALD measurements of the other proteins.

Considering these pol ϵ ALD results together, we propose that loading of pol ϵ onto PCNA is mainly dependent on the alternative clamp loader complex CHTF18-RFC.

DISCUSSION

Our results have revealed an unexpected complexity in repair synthesis in human cells. Approximately 50% of the repair synthesis used polk recruited by ubiquitinated PCNA and XRCC1, together with pol δ recruited by the classical RFC complex. The remaining 50% is carried out by pol ϵ recruited by the CHTF18-RFC complex. We propose the following model to explain our findings. RAD18 accumulates at sites of UV damage very rapidly and independently of NER-mediated dual incision (Figure 6A) ((Nakajima et al., 2006) and our unpublished data). Ubiquitination of pre-loaded PCNA and repositioning of PCNA to the site of the lesion may therefore occur before completion of the pre-incision complex assembly (Figure 6B). In support of this suggestion, we have been able to detect low levels of ALD of PCNA (but not of pol δ) in several NER-deficient XP primary fibroblasts (unpublished data of J Moser, RMO and MIF). Our results delineate two pathways for repair synthesis, following incision, one dependent on pol ϵ , the other requiring both pol δ and polk. One possibility is that the former deals with damage on the leading strand, the latter on the lagging strand. We consider this unlikely since most of our assays involve analysis of cells that were not replicating their DNA. A more likely explanation is that different mechanisms are used to deal with different conformations of the repair sites or of the chromatin structure around the damaged sites. We suggest that 50% of the sites are in an accessible configuration and pol ϵ can carry out repair synthesis rapidly (Figures 6C1~6E1). In mode 1, pol ϵ recruitment by CHTF18-RFC occurs following conventional dual incision; possibly, recruitment of polymerases δ and κ might be inhibited (Figure 6C1~6D1). After completion of repair synthesis, release of pol ϵ and recruitment of LigI occur (Figure 6E1).

In the second pathway, for example because of the conformation of the repair site or the chromatin structure, repair synthesis is more difficult, resulting in 3' incision being delayed relative to 5' incision (Figure 6C2). This causes displacement synthesis, as was also proposed in early studies (Mullenders et al., 1985; Smith and Okumoto, 1984) and is consistent with the recent finding that XPF cleaves on the 5' side of the damage prior to cleavage on the 3' side by XPG, thereby leaving a 5' flap to be displaced (Staresincic et al., 2009). This 2nd mode (Figures 6C2~6E2) has more rigid requirements because of the surrounding steric hindrance; this mode involves both pol δ and polk. Recruitment of pol δ occurs independently of PCNA ubiquitination status, but does depend on its accessory p66 subunit as well as the RFC complex (Figure 6C2), whereas recruitment of polk requires XRCC1 as well as ubiquitination of PCNA (Figure 6D2). Hydroxyurea prevents completion of repair synthesis, resulting in an accumulation of repair synthesis intermediates, perhaps because of displacement synthesis as suggested earlier (Mullenders et al., 1985; Smith and Okumoto, 1984), and an increased ALD of repair synthesis proteins.

XRCC1 appears to have a fairly direct, as yet undefined, role in recruiting polk, and, after completion of repair synthesis, release of polymerases from the repair-patch and XRCC1 dependent recruitment of LigIII occur (Figure 6E2). Our data are consistent with a recent report suggesting that *in vitro* pol δ is rather distributive, even in the presence of PCNA, whereas RFC remains at the primer-terminus (Masuda et al., 2007). Which of the polymerases operates first in mode 2 and why both are needed will be the subject of future studies.

The major function of Y-family DNA polymerases is believed to be in translesion synthesis (TLS), the bypass of DNA lesions that block replication by normal replicative DNA polymerases (Prakash et al., 2005). Because of this property, the replication fidelities of the Y-family enzymes are very low (McCulloch and Kunkel, 2008). Polk is specialised for TLS past bulky DNA lesions (Avkin et al., 2004; Ohashi et al., 2000b; Suzuki et al., 2002) and induces mutations when it acts on undamaged templates with a frequency of about 10^{-3} (Ohashi et al., 2000a; Zhang et al., 2000). We have considered the possibility that when there are two closely spaced lesions on opposite strands, repair synthesis on one strand will need to bypass the lesion on the opposite strand, and that the role of polk is to carry out this TLS step. Lam and Reynolds carried out a detailed analysis of the frequency of closely spaced lesions in human fibroblasts (Lam and Reynolds, 1986). After a dose of 40 J/m^{-2} used in our ALD experiments, they found that the proportion of overlapping lesions ($0.8/10^8$ daltons) represented only 0.5% of the total lesions ($1.5/10^6$ daltons). We think that this is unlikely to explain our data. There is increasing evidence that apart from their roles in TLS, Y-family polymerases have other functions as well (reviewed in (Lehmann, 2006)). At first sight it may seem strange that the cell uses an error-prone polymerase to carry out NER repair synthesis. However we have previously speculated that the low K_m of polk may make it especially suitable for use under conditions of low nucleotide concentration (Ogi and Lehmann, 2006). An error frequency of 10^{-3} together with a patch size of 30 nucleotides would result in about 1 error every 30 repair patches. This may be a price worth paying for the cell to carry out successful repair synthesis. We speculate that polk may in this way contribute to UV-induced mutagenesis in normal human cells, especially in quiescence. Indeed, the bacterial homologue of polk, DinB, is believed to be involved in untargeted mutagenesis

in *E.coli*, a mutagenic process that occurs on non-damaged DNA templates - independently of TLS- under conditions of starvation (Brotcorne-Lannoye and Maenhaut-Michel, 1986).

Our results, though raising many new questions, give important novel insights into the complexity of repair synthesis and the role of different polymerases in this process.

EXPERIMENTAL PROCEDURES

All the experimental procedures are described in Supplemental Data.

ACKNOWLEDGEMENTS

This work was supported by Special Coordination Funds for Promoting Science and Technology from Japan Science and Technology Agency, a Grant in aid for Scientific Research KAKENHI (20810021) from Japan Society for the Promotion of Science, and a Butterfield Medical Award from the Great Britain Sasakawa Foundation to TO; a Global COE Program from the Ministry of Education, Culture, Sports, Sciences and Technology of Japan to TO, SL, YN and SY; a KAKENHI to KT and YM; an MRC programme grant to ARL, an EC-RTN and integrated project to ARL and LM. We are grateful to Ms. Yumi Gushiken for anti-polk antibody purification. The anti-pole antibody, 3A3.2, is a kind gift from Dr. Stuart Linn (UC Berkeley, USA).

Figure legends

Figure 1 UVC irradiation dependent PCNA ubiquitination in quiescent cells and interaction of DNA polymerases with NER post-incision machinery.

(A-C) Western blot showing ubiquitination of PCNA at indicated times after (A, B) 20 J/m² global UVC irradiation, or (C) 10 mM hydroxyurea (HU) treatment in quiescent cells. Normal (48BR), XPA (XP15BR), and XPC (XP21BR) are all quiescent primary fibroblasts (G0). -, without treatment. SV40 transformed MRC5 cells (MRC5V1) were used as a control. In B, cells were extracted with tritonX100 before harvesting (Tx). (D-H) Normal (VH25) or XPA (XP25RO) primary fibroblasts that were either serum-starved (G0) or close to confluent density (Cycling) were globally UVC-irradiated (20 J/m²) and incubated for 1h. Repair proteins were then cross-linked to DNA with formaldehyde treatment followed by ChIP with (D-F) mouse anti-PCNA, PC-10 antibody, (G) rabbit anti-polk, K1 antibody, or (H) mouse anti-XRCC1, 33-2-5 antibody. Co-precipitated proteins were analysed by western blotting with the antibodies listed in Supplementary data. **See also Supplementary Figure S1.**

Figure 2 Polk accumulation at local damage is dependent on early steps of NER

(A, B) non-dividing normal 48BR human primary fibroblasts were transfected with either (A) *siNTC* non-targeting control or (B) *POLK* targeting siRNA, UVC-irradiated (40 J/m²) through a polycarbonate (PC) micropore filter (5µm), followed by 30 min incubation with 10 mM hydroxyurea (HU) and immunostaining with mouse anti-RPA70 (RPA70-9, green), and rabbit anti-polk (K1, red) antibodies. Blue, DAPI stain. (C) XP15BR XP-A cells were cocultured with normal 48BR cells containing blue

beads (Ctr), UVC-irradiated and processed as in (A), except that the post UVC incubation was for 1 h without HU. The insets in this and subsequent figures show enlarged images of individual cells. In C the inset in the white box is a normal cell, in the red box an XP cell. [See also Supplementary Figure S2.](#)

Figure 3 Role of polk in NER is dependent on PCNA ubiquitination

(A) siRNA knockdown of RAD18 diminishes the ALD of polk but not pol δ . Cells incubated with blue beads and siRNA non-targeting control were cocultivated with cells incubated with *RAD18* siRNA, and locally UVC irradiated (5 μ m pores, 40 J/m²), followed by 1h incubation without inhibitors. White arrows indicate pol δ (p125, green) and polk (red) double positive nuclei in cells treated with non-targeting control (also in inset in white box), whereas green arrows indicate nuclei with pol δ spots only in cells treated with *RAD18* siRNA (also shown in inset in red box). (B) Western blot showing that siRNA knockdown of RAD18 abolishes PCNA ubiquitination. Normal 48BR primary fibroblasts (left) or normal but SV40 immortalised MRC5VI cells (right) were transfected with either *siNTC* non-targeting control (*NTC*) or *RAD18* targeting (*R18*) siRNA and cultured at close to confluent density. Cells were globally UVC irradiated (10J/m²), followed by incubation for 1h without inhibitors. RAD18 and the ubiquitinated PCNA were respectively detected by rabbit anti-RAD18 (ab19937, Abcam), and mouse anti-PCNA (PC-10) antibodies. Asterisks indicate non-specific bands. (C) ALD of indicated NER proteins in 48BR cells depleted of RAD18 or polk using siRNAs. Cells were locally UVC irradiated as in (A). % ALD represents the relative percentage of cells showing ALD of the indicated protein above a predetermined threshold compared with the percentage in relevant controls. Bars and error bars indicate respectively averages and standard deviations calculated from at

least three independent experiments. (D) ALD of wild-type or indicated mutants of polk. SV40 transformed MRC5 cells were transfected with plasmid expressing GFP-tagged either wild type human *POLK*, or *POLK* with UBZ mutations at indicated amino acid positions (GFP-POLK, green; [see also Supplementary Figure S2K](#)). Cells were locally UVC irradiated as in (A), followed by immunostaining with anti-RPA antibody (RPA70-9, red). (E) Effect of RAD18 and polk depletion on UDS. 48BR cells were transfected with indicated siRNAs, UVC-irradiated (10 J/m^2) followed by EdU incorporation for 2h. Bars and error bars respectively indicate averages and standard deviations of nuclear fluorescent intensity measured in at least 250 nuclei from at least 5 different positions. [See also Supplementary Figure S3](#).

Figure 4 Effects of DNA polymerase knockdowns on UDS and ALD.

(A) ALD of pol δ p125 (A-9 antibody; top and bottom, green), p66 (3E2 antibody; middle, green) and polk (K1 antibody; bottom, red) in primary 48BR cells treated with the indicated siRNA and locally UVC-irradiated (40 J/m^2) followed by 30 min incubation. In the top and middle panels, white arrows represent nuclei with spots of indicated pol δ subunit, whereas in the bottom panel, green and red arrows indicate nuclei with pol δ p125 and polk spots, respectively. Note that smaller sized green spots seen in the bottom panels are nonspecific nucleoli staining. (B) Histogram analyses are shown. Bars and error bars indicate respectively averages and standard deviations of the percentages of ALD calculated from at least three independent experiments shown in (A). (C, D, E) Effects of multiple DNA polymerase knockdowns on UDS. 48BR cells were transfected with indicated siRNAs, UVC-irradiated (10 J/m^2) followed by EdU incorporation for 2h. Bars and error bars

respectively indicate averages and standard deviations of nuclear fluorescent intensity measured in at least 250 nuclei from at least 5 different positions.

Figure 5 Differential requirement of repair replication factors for recruitment of gap-filling DNA polymerases.

(A) ALD of pol δ p125, p66 and polk in 48BR cells depleted of indicated genes using siRNAs and local UVC-irradiation (40 J/m²) followed by 1h incubation without inhibitors. Bars and error bars indicate respectively averages and standard deviations of the percentages of ALD calculated from at least three independent experiments. (B) Depletion of RFC1 abolishes pol δ ALD but does not affect polk ALD. Cells with non-targeted siRNA cultured with blue beads were cocultured with cells in which RFC1 was depleted by siRNA. White arrow indicates pol δ (p125, green) and polk (red) double positive nuclei, whereas red arrows indicate nuclei with polk spots only. KD, knockdown (also inset with red box); Ctr, Control (also inset in white box). (C) Depletion of XRCC1 abolishes polk ALD but does not affect pol δ ALD. White arrows indicate pol δ (p125, green) and polk (red) double positive nuclei, whereas green arrows indicate nuclei with pol δ spots only. (D) UDS following depletion of indicated genes. 48BR cells were transfected with indicated siRNAs, UVC-irradiated (10 J/m²) followed by EdU incorporation for 2h. Bars and error bars respectively indicate averages and standard deviations of nuclear fluorescent intensity measured in at least 250 nuclei from at least 5 different positions. (E) ALD of pol ϵ in 48BR cells depleted of indicated genes using siRNAs. Cells were pre-fixed before immunostaining, as described in Figure S4. Bars and error bars indicate respectively averages and standard deviations of the percentages of ALD calculated from at least three independent experiments. (F) Depletion of CHTF18 inhibits pol ϵ ALD. Cells

with non-targeted siRNA cultured with blue beads were cocultured with cells in which CHTF18 was depleted by siRNA. As described in Figure S4, cells were pre-fixed before immunostaining. White arrow indicates pol ϵ (green) and XPB (red) double positive nuclei, whereas red arrows indicate nuclei with XPB spots only. Neg, pol ϵ negative non-cycling cells.

Figure 6 Model for action of pol κ and pol δ during NER gap-filling DNA

synthesis. (A) Section of chromatin in quiescent cells with PCNA loaded on the DNA and damage sensed by Rad18, which is then able to ubiquitinate PCNA. (B) Assembly of the pre-incision complex. (C1-E1) In mode 1, following dual incisions to release the damaged fragment (C1), pol ϵ is recruited by CHTF18-RFC to fill the gap (D1) followed by Ligase I recruitment to seal the nick (E1). (C2-E2) In mode 2, 5' incision is followed by recruitment of both pol δ core by RFC and p66 (C2) and pol κ /XRCC1 by ubiquitinated PCNA (D2). (E2) After completion of repair synthesis, pol κ is released, XPG cleaves off the flap and XRCC1 recruits Ligase III to seal the remaining nick.

REFERENCES

Aboussekhra, A., Biggerstaff, M., Shivji, M.K., Vilpo, J.A., Moncollin, V., Podust, V.N., Protic, M., Hubscher, U., Egly, J.M., and Wood, R.D. (1995). Mammalian DNA nucleotide excision repair reconstituted with purified protein components. *Cell* 80, 859-868.

Andressoo, J.O., and Hoeijmakers, J.H. (2005). Transcription-coupled repair and premature ageing. *Mutat Res* 577, 179-194.

Araujo, S.J., Tirode, F., Coin, F., Pospiech, H., Syvaaja, J.E., Stucki, M., Hubscher, U., Egly, J.M., and Wood, R.D. (2000). Nucleotide excision repair of DNA with recombinant human proteins: definition of the minimal set of factors, active forms of TFIIH, and modulation by CAK. *Genes Dev* 14, 349-359.

Avkin, S., Goldsmith, M., Velasco-Miguel, S., Geacintov, N., Friedberg, E.C., and Livneh, Z. (2004). Quantitative analysis of translesion DNA synthesis across a benzo[a]pyrene-guanine adduct in mammalian cells: the role of DNA polymerase kappa. *J Biol Chem* 279, 53298-53305.

Bermudez, V.P., Maniwa, Y., Tappin, I., Ozato, K., Yokomori, K., and Hurwitz, J. (2003). The alternative Ctf18-Dcc1-Ctf8-replication factor C complex required for sister chromatid cohesion loads proliferating cell nuclear antigen onto DNA. *Proc Natl Acad Sci U S A* 100, 10237-10242.

Bi, X., Barkley, L.R., Slater, D.M., Tateishi, S., Yamaizumi, M., Ohmori, H., and Vaziri, C. (2006). Rad18 regulates DNA polymerase kappa and is required for recovery from S-phase checkpoint-mediated arrest. *Mol Cell Biol* 26, 3527-3540.

Bienko, M., Green, C.M., Crosetto, N., Rudolf, F., Zapart, G., Coull, B., Kannouche, P., Wider, G., Peter, M., Lehmann, A.R., *et al.* (2005). Ubiquitin-binding domains in Y-family polymerases regulate translesion synthesis. *Science* 310, 1821-1824.

Brotcorne-Lannoye, A., and Maenhaut-Michel, G. (1986). Role of RecA protein in untargeted UV mutagenesis of bacteriophage lambda: evidence for the requirement for the dinB gene. *Proc Natl Acad Sci U S A* 83, 3904-3908.

Ducoux, M., Urbach, S., Baldacci, G., Hubscher, U., Koundrioukoff, S., Christensen, J., and Hughes, P. (2001). Mediation of proliferating cell nuclear antigen (PCNA)-

dependent DNA replication through a conserved p21(Cip1)-like PCNA-binding motif present in the third subunit of human DNA polymerase delta. *J Biol Chem* 276, 49258-49266.

Fousteri, M., Vermeulen, W., van Zeeland, A.A., and Mullenders, L.H. (2006). Cockayne syndrome A and B proteins differentially regulate recruitment of chromatin remodeling and repair factors to stalled RNA polymerase II in vivo. *Mol Cell* 23, 471-482.

Friedberg, E.C., Lehmann, A.R., and Fuchs, R.P. (2005a). Trading places: how do DNA polymerases switch during translesion DNA synthesis? *Mol Cell* 18, 499-505.

Friedberg, E.C., Walker, G.C., Siede, W., Wood, R.D., Schultz, R.A., and Ellenberger, T. (2005b). *DNA Repair and Mutagenesis*, 2 edn (ASM Press).

Gerik, K.J., Li, X., Pautz, A., and Burgers, P.M. (1998). Characterization of the two small subunits of *Saccharomyces cerevisiae* DNA polymerase delta. *J Biol Chem* 273, 19747-19755.

Gibbs, P.E., McDonald, J., Woodgate, R., and Lawrence, C.W. (2005). The relative roles in vivo of *Saccharomyces cerevisiae* Pol eta, Pol zeta, Rev1 protein and Pol32 in the bypass and mutation induction of an abasic site, T-T (6-4) photoadduct and T-T cis-syn cyclobutane dimer. *Genetics* 169, 575-582.

Gillet, L.C., and Scharer, O.D. (2006). Molecular mechanisms of mammalian global genome nucleotide excision repair. *Chem Rev* 106, 253-276.

Guo, C., Tang, T.S., Bienko, M., Dikic, I., and Friedberg, E.C. (2008). Requirements for the interaction of mouse Polkappa with ubiquitin and its biological significance. *J Biol Chem* 283, 4658-4664.

Hanawalt, P.C., and Spivak, G. (2008). Transcription-coupled DNA repair: two decades of progress and surprises. *Nat Rev Mol Cell Biol* 9, 958-970.

Hanna, J.S., Kroll, E.S., Lundblad, V., and Spencer, F.A. (2001). *Saccharomyces cerevisiae* CTF18 and CTF4 are required for sister chromatid cohesion. *Mol Cell Biol* 21, 3144-3158.

Hoege, C., Pfander, B., Moldovan, G.L., Pyrowolakis, G., and Jentsch, S. (2002). RAD6-dependent DNA repair is linked to modification of PCNA by ubiquitin and SUMO. *Nature* 419, 135-141.

Hughes, P., Tratner, I., Ducoux, M., Piard, K., and Baldacci, G. (1999). Isolation and identification of the third subunit of mammalian DNA polymerase delta by PCNA-affinity chromatography of mouse FM3A cell extracts. *Nucleic Acids Res* 27, 2108-2114.

Johnson, A., and O'Donnell, M. (2005). Cellular DNA replicases: components and dynamics at the replication fork. *Annu Rev Biochem* 74, 283-315.

Kai, M., and Wang, T.S. (2003). Checkpoint activation regulates mutagenic translesion synthesis. *Genes Dev* 17, 64-76.

Kannouche, P.L., Wing, J., and Lehmann, A.R. (2004). Interaction of human DNA polymerase eta with monoubiquitinated PCNA: a possible mechanism for the polymerase switch in response to DNA damage. *Mol Cell* 14, 491-500.

Lam, L.H., and Reynolds, R.J. (1986). A sensitive, enzymatic assay for the detection of closely opposed cyclobutyl pyrimidine dimers induced in human diploid fibroblasts. *Mutat Res* 166, 187-198.

Lee, M.Y., Jiang, Y.Q., Zhang, S.J., and Toomey, N.L. (1991). Characterization of human DNA polymerase delta and its immunochemical relationships with DNA polymerase alpha and epsilon. *J Biol Chem* 266, 2423-2429.

Lehmann, A.R. (2006). New functions for Y family polymerases. *Mol Cell* 24, 493-495.

Lehmann, A.R., Niimi, A., Ogi, T., Brown, S., Sabbioneda, S., Wing, J.F., Kannouche, P.L., and Green, C.M. (2007). Translesion synthesis: Y-family polymerases and the polymerase switch. *DNA Repair (Amst)* 6, 891-899.

Limsirichaikul, S., Niimi, A., Fawcett, H., Lehmann, A., Yamashita, S., and Ogi, T. (2009). A rapid non-radioactive technique for measurement of repair synthesis in primary human fibroblasts by incorporation of ethynyl deoxyuridine (EdU). *Nucleic Acids Res* 37, e31.

Majka, J., and Burgers, P.M. (2004). The PCNA-RFC families of DNA clamps and clamp loaders. *Prog Nucleic Acid Res Mol Biol* 78, 227-260.

Masuda, Y., Suzuki, M., Piao, J., Gu, Y., Tsurimoto, T., and Kamiya, K. (2007). Dynamics of human replication factors in the elongation phase of DNA replication. *Nucleic Acids Res* 35, 6904-6916.

McCulloch, S.D., and Kunkel, T.A. (2008). The fidelity of DNA synthesis by eukaryotic replicative and translesion synthesis polymerases. *Cell Res* 18, 148-161.

Moldovan, G.L., Pfander, B., and Jentsch, S. (2007). PCNA, the maestro of the replication fork. *Cell* 129, 665-679.

Moser, J., Kool, H., Giakzidis, I., Caldecott, K., Mullenders, L.H., and Foustieri, M.I. (2007). Sealing of chromosomal DNA nicks during nucleotide excision repair requires XRCC1 and DNA ligase III alpha in a cell-cycle-specific manner. *Mol Cell* 27, 311-323.

Mullenders, L.H., van Kesteren-van Leeuwen, A.C., van Zeeland, A.A., and Natarajan, A.T. (1985). Analysis of the structure and spatial distribution of ultraviolet-induced DNA repair patches in human cells made in the presence of inhibitors of replicative synthesis. *Biochim Biophys Acta* 826, 38-48.

Nakajima, S., Lan, L., Kanno, S., Usami, N., Kobayashi, K., Mori, M., Shiomi, T., and Yasui, A. (2006). Replication-dependent and -independent responses of RAD18 to DNA damage in human cells. *J Biol Chem* 281, 34687-34695.

Nishida, C., Reinhard, P., and Linn, S. (1988). DNA repair synthesis in human fibroblasts requires DNA polymerase delta. *J Biol Chem* 263, 501-510.

Ogi, T., Kannouche, P., and Lehmann, A.R. (2005). Localisation of human Y-family DNA polymerase kappa: relationship to PCNA foci. *J Cell Sci* 118, 129-136.

Ogi, T., and Lehmann, A.R. (2006). The Y-family DNA polymerase kappa (pol kappa) functions in mammalian nucleotide-excision repair. *Nat Cell Biol* 8, 640-642.

Ogiwara, H., Ohuchi, T., Ui, A., Tada, S., Enomoto, T., and Seki, M. (2007). Ctf18 is required for homologous recombination-mediated double-strand break repair. *Nucleic Acids Res* 35, 4989-5000.

Ohashi, E., Bebenek, K., Matsuda, T., Feaver, W.J., Gerlach, V.L., Friedberg, E.C., Ohmori, H., and Kunkel, T.A. (2000a). Fidelity and processivity of DNA synthesis by DNA polymerase kappa, the product of the human DINB1 gene. *J Biol Chem* 275, 39678-39684.

Ohashi, E., Ogi, T., Kusumoto, R., Iwai, S., Masutani, C., Hanaoka, F., and Ohmori, H. (2000b). Error-prone bypass of certain DNA lesions by the human DNA polymerase kappa. *Genes Dev* 14, 1589-1594.

Ohmori, H., Friedberg, E.C., Fuchs, R.P., Goodman, M.F., Hanaoka, F., Hinkle, D., Kunkel, T.A., Lawrence, C.W., Livneh, Z., Nohmi, T., *et al.* (2001). The Y-family of DNA polymerases. *Mol Cell* 8, 7-8.

Plosky, B.S., Vidal, A.E., Fernandez de Henestrosa, A.R., McLenigan, M.P., McDonald, J.P., Mead, S., and Woodgate, R. (2006). Controlling the subcellular

localization of DNA polymerases iota and eta via interactions with ubiquitin. *EMBO J* 25, 2847-2855.

Podust, V.N., Chang, L.S., Ott, R., Dianov, G.L., and Fanning, E. (2002).

Reconstitution of human DNA polymerase delta using recombinant baculoviruses: the p12 subunit potentiates DNA polymerizing activity of the four-subunit enzyme. *J Biol Chem* 277, 3894-3901.

Prakash, S., Johnson, R.E., and Prakash, L. (2005). Eukaryotic translesion synthesis DNA polymerases: specificity of structure and function. *Annu Rev Biochem* 74, 317-353.

Shikata, K., Ohta, S., Yamada, K., Obuse, C., Yoshikawa, H., and Tsurimoto, T. (2001). The human homologue of fission Yeast *cdc27*, p66, is a component of active human DNA polymerase delta. *J Biochem* 129, 699-708.

Shiomi, Y., Masutani, C., Hanaoka, F., Kimura, H., and Tsurimoto, T. (2007). A second proliferating cell nuclear antigen loader complex, Ctf18-replication factor C, stimulates DNA polymerase eta activity. *J Biol Chem* 282, 20906-20914.

Smith, C.A., and Okumoto, D.S. (1984). Nature of DNA repair synthesis resistant to inhibitors of polymerase alpha in human cells. *Biochemistry* 23, 1383-1391.

Staresincic, L., Fagbemi, A.F., Enzlin, J.H., Gourdin, A.M., Wijgers, N., Dunand-Sauthier, I., Giglia-Mari, G., Clarkson, S.G., Vermeulen, W., and Scharer, O.D. (2009). Coordination of dual incision and repair synthesis in human nucleotide excision repair. *EMBO J* 28, 1111-1120.

Suzuki, N., Ohashi, E., Kolbanovskiy, A., Geacintov, N.E., Grollman, A.P., Ohmori, H., and Shibutani, S. (2002). Translesion synthesis by human DNA polymerase kappa on a DNA template containing a single stereoisomer of dG-(+)- or dG-(-)-anti-N(2)-

BPDE (7,8-dihydroxy-anti-9,10-epoxy-7,8,9,10-tetrahydrobenzo[a]pyrene).
Biochemistry 41, 6100-6106.

Volker, M., Mone, M.J., Karmakar, P., van Hoffen, A., Schul, W., Vermeulen, W.,
Hoeijmakers, J.H., van Driel, R., van Zeeland, A.A., and Mullenders, L.H. (2001).
Sequential assembly of the nucleotide excision repair factors in vivo. *Mol Cell* 8, 213-
224.

Watanabe, K., Tateishi, S., Kawasuji, M., Tsurimoto, T., Inoue, H., and Yamaizumi,
M. (2004). Rad18 guides poleta to replication stalling sites through physical
interaction and PCNA monoubiquitination. *EMBO J* 23, 3886-3896.

Wood, R.D., and Shivji, M.K. (1997). Which DNA polymerases are used for DNA-
repair in eukaryotes? *Carcinogenesis* 18, 605-610.

Zhang, Y., Yuan, F., Xin, H., Wu, X., Rajpal, D.K., Yang, D., and Wang, Z. (2000).
Human DNA polymerase kappa synthesizes DNA with extraordinarily low fidelity.
Nucleic Acids Res 28, 4147-4156.

Zhou, J.Q., He, H., Tan, C.K., Downey, K.M., and So, A.G. (1997). The small subunit
is required for functional interaction of DNA polymerase delta with the proliferating
cell nuclear antigen. *Nucleic Acids Res* 25, 1094-1099.

Figure1
[Click here to download high resolution image](#)

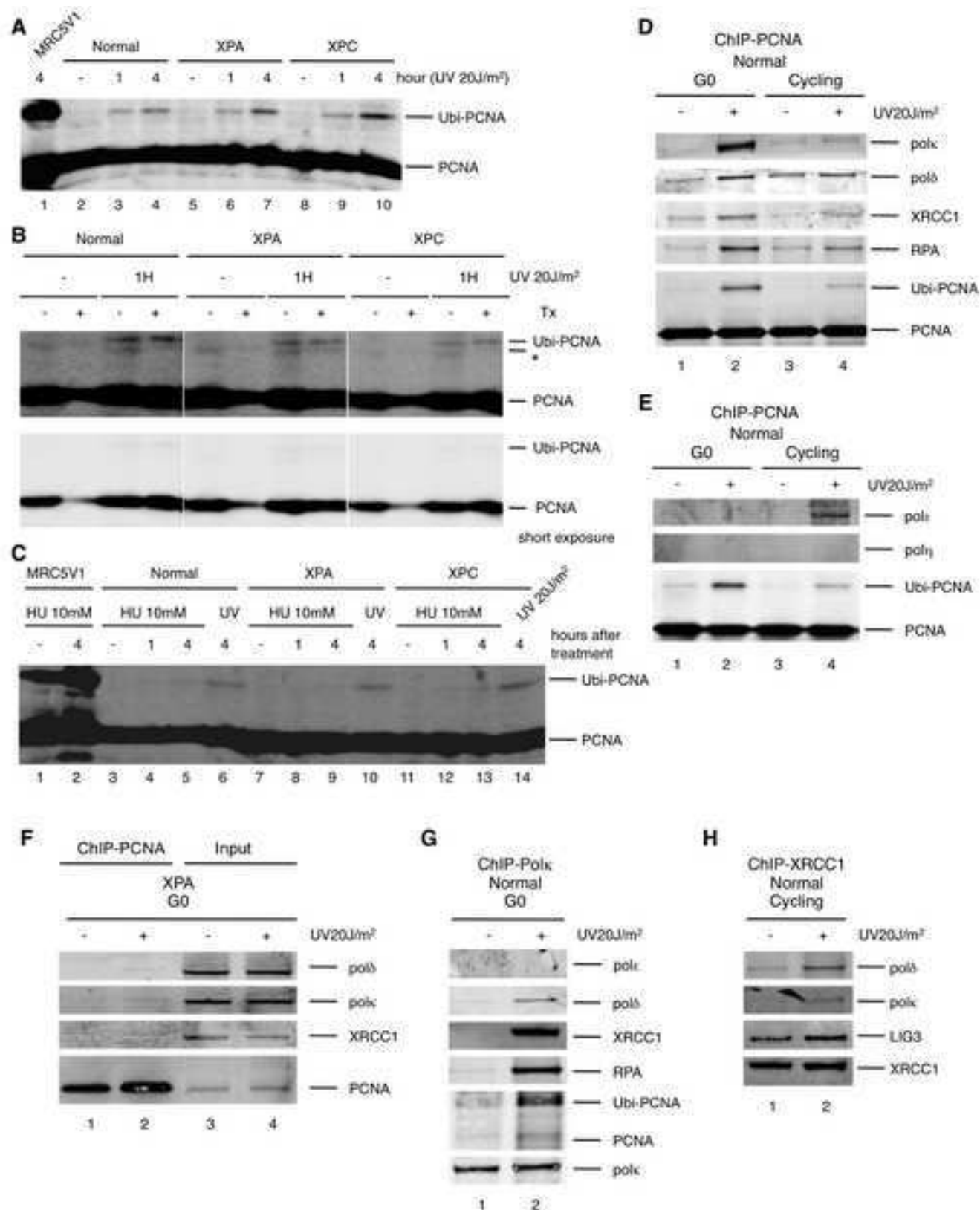


Figure 1

Figure2
[Click here to download high resolution image](#)

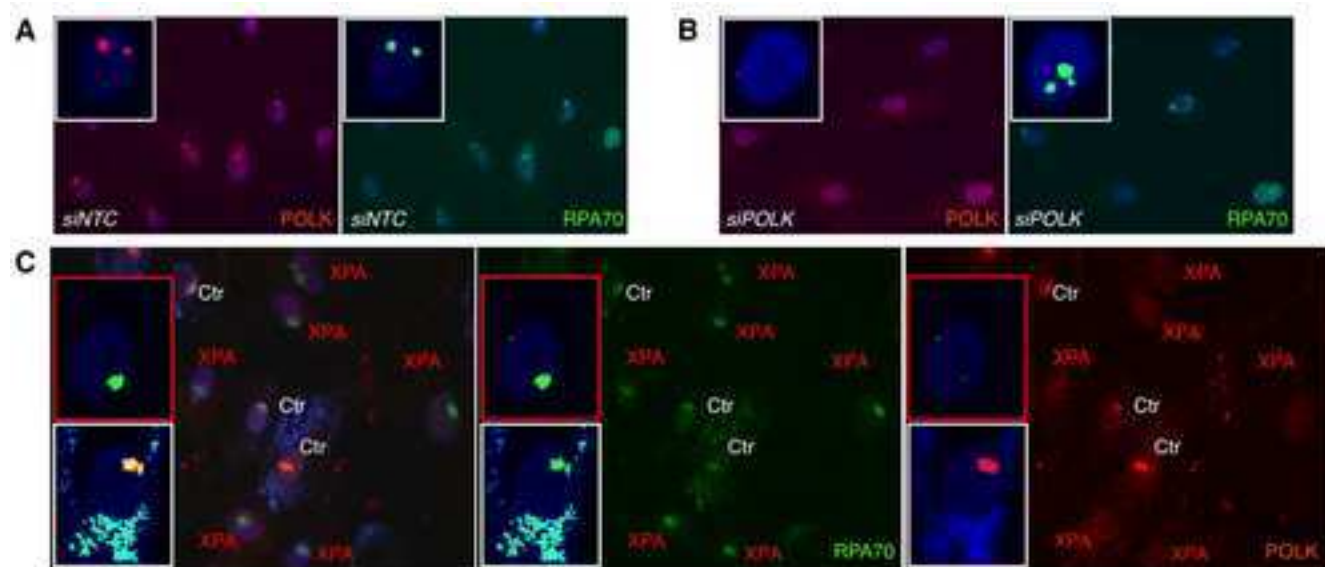


Figure 2

Figure3
[Click here to download high resolution image](#)

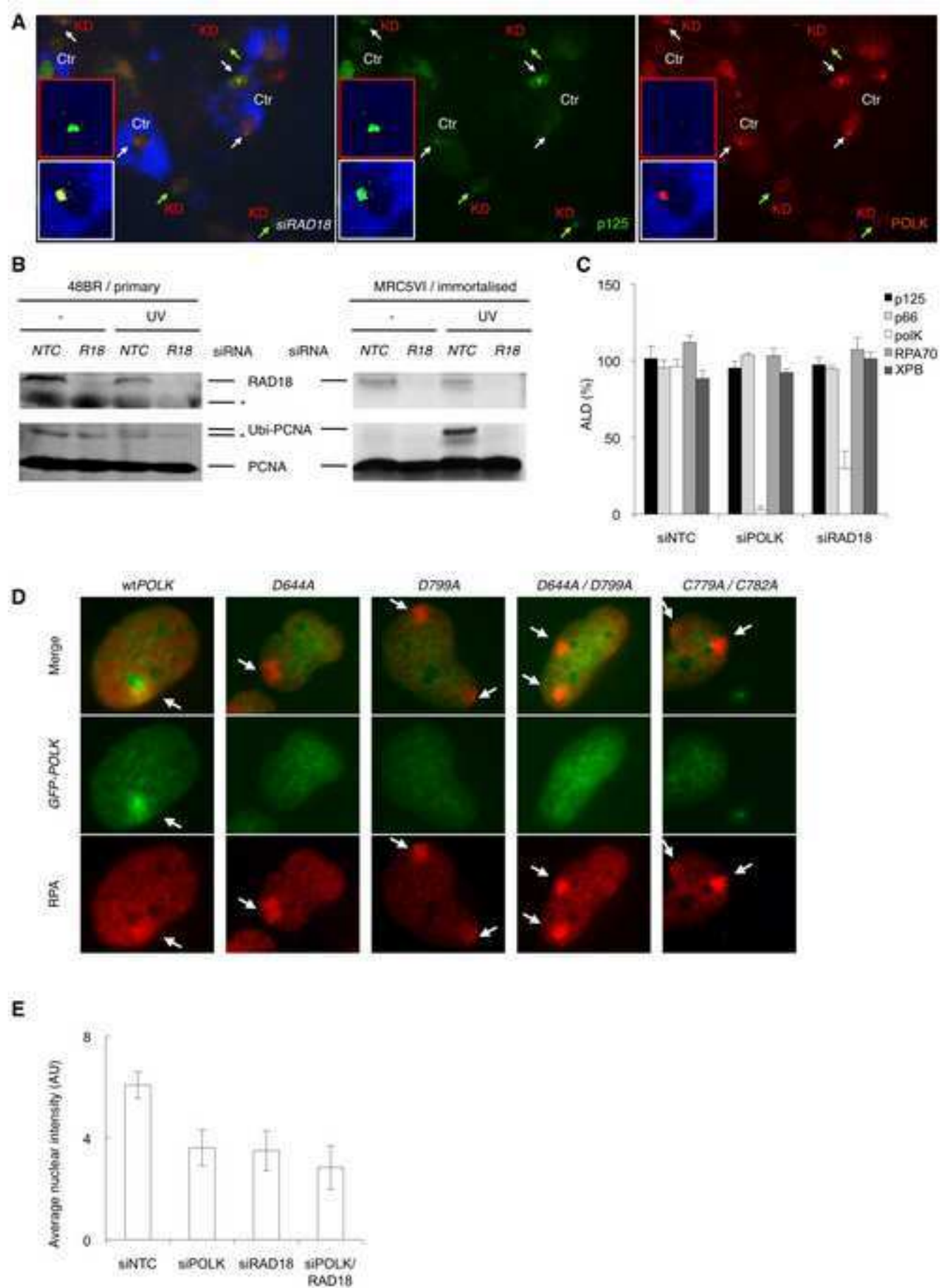


Figure 3

Figure4
[Click here to download high resolution image](#)

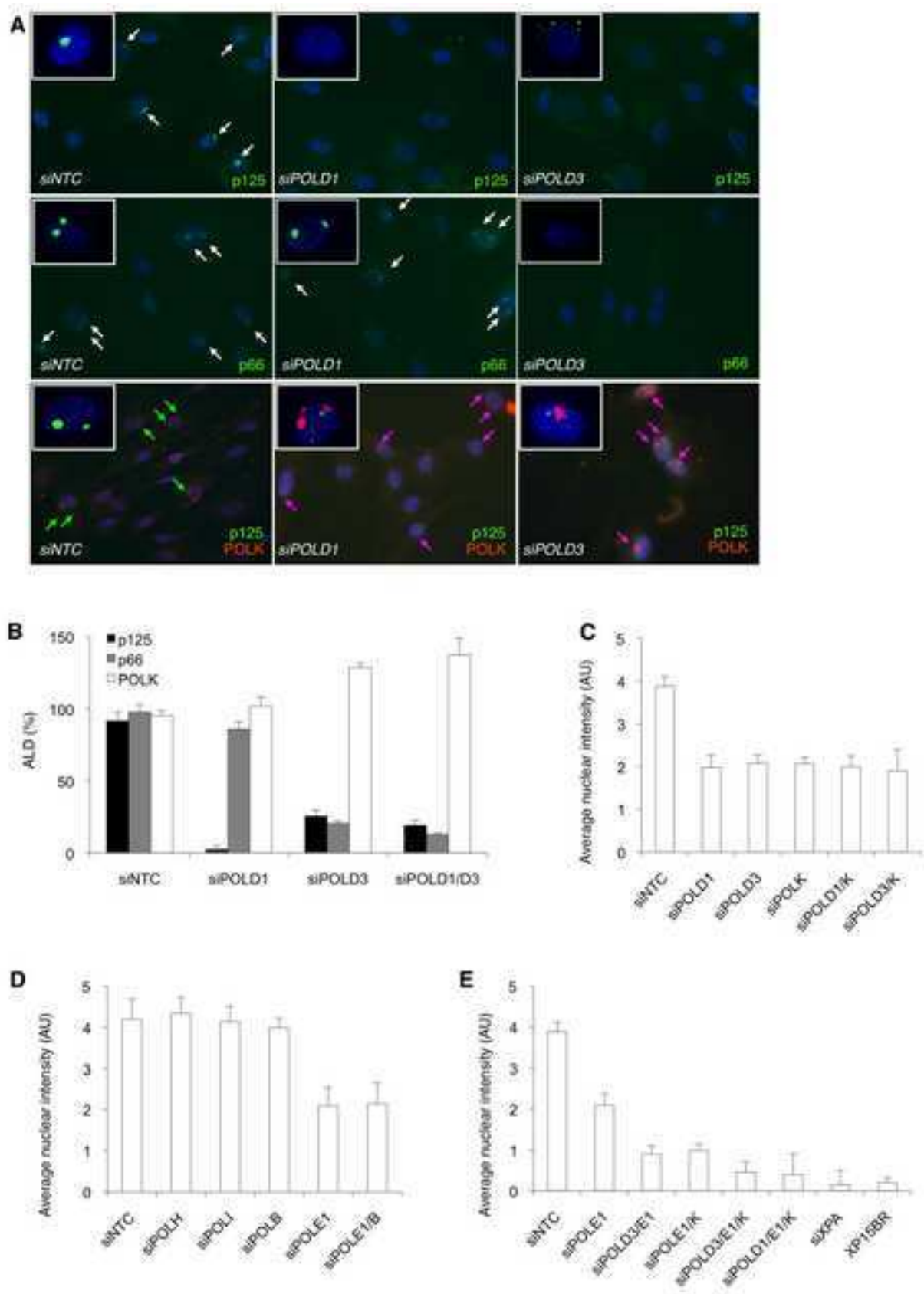


Figure 4

Figure5
[Click here to download high resolution image](#)

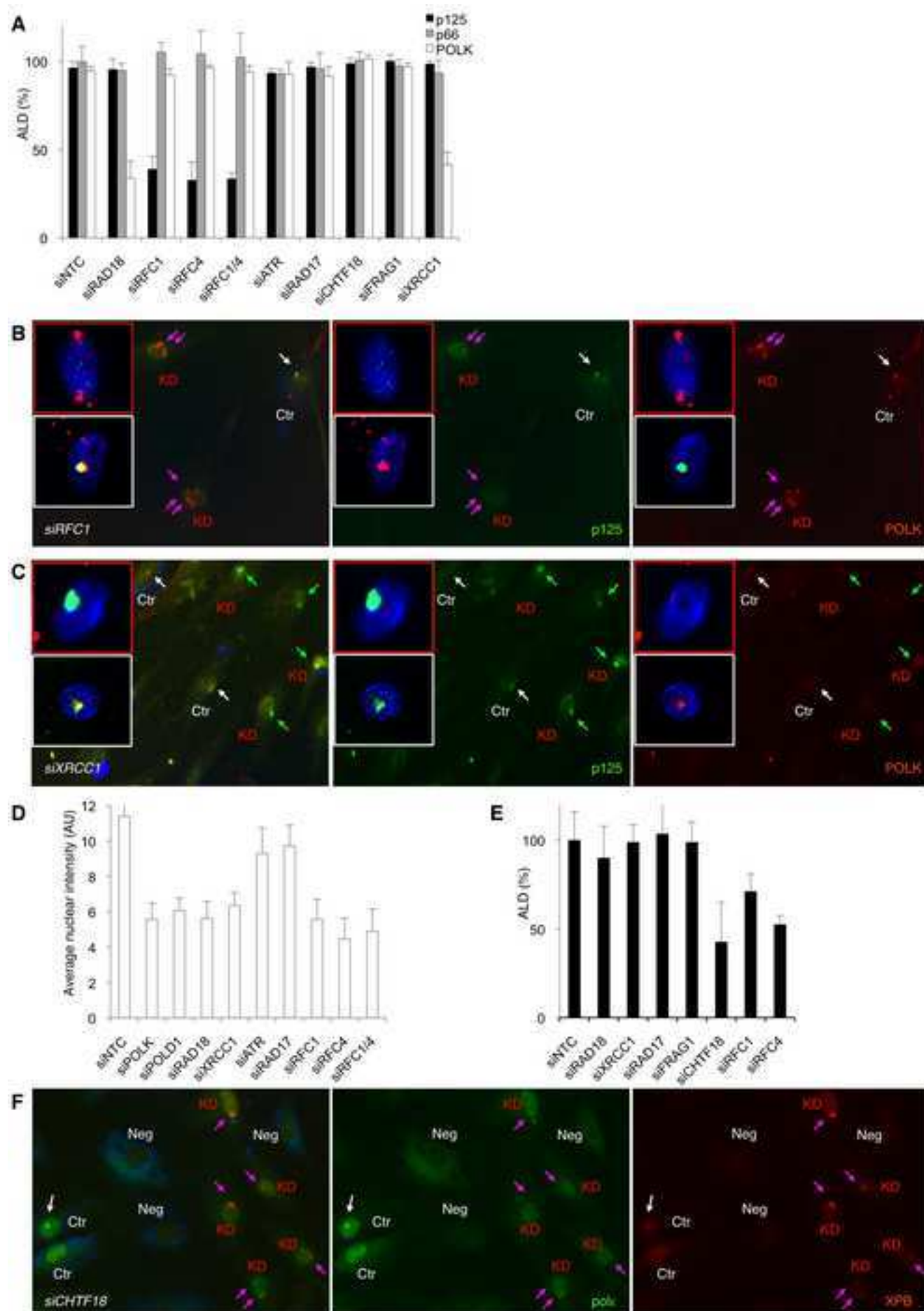


Figure 5

Figure6
[Click here to download high resolution image](#)

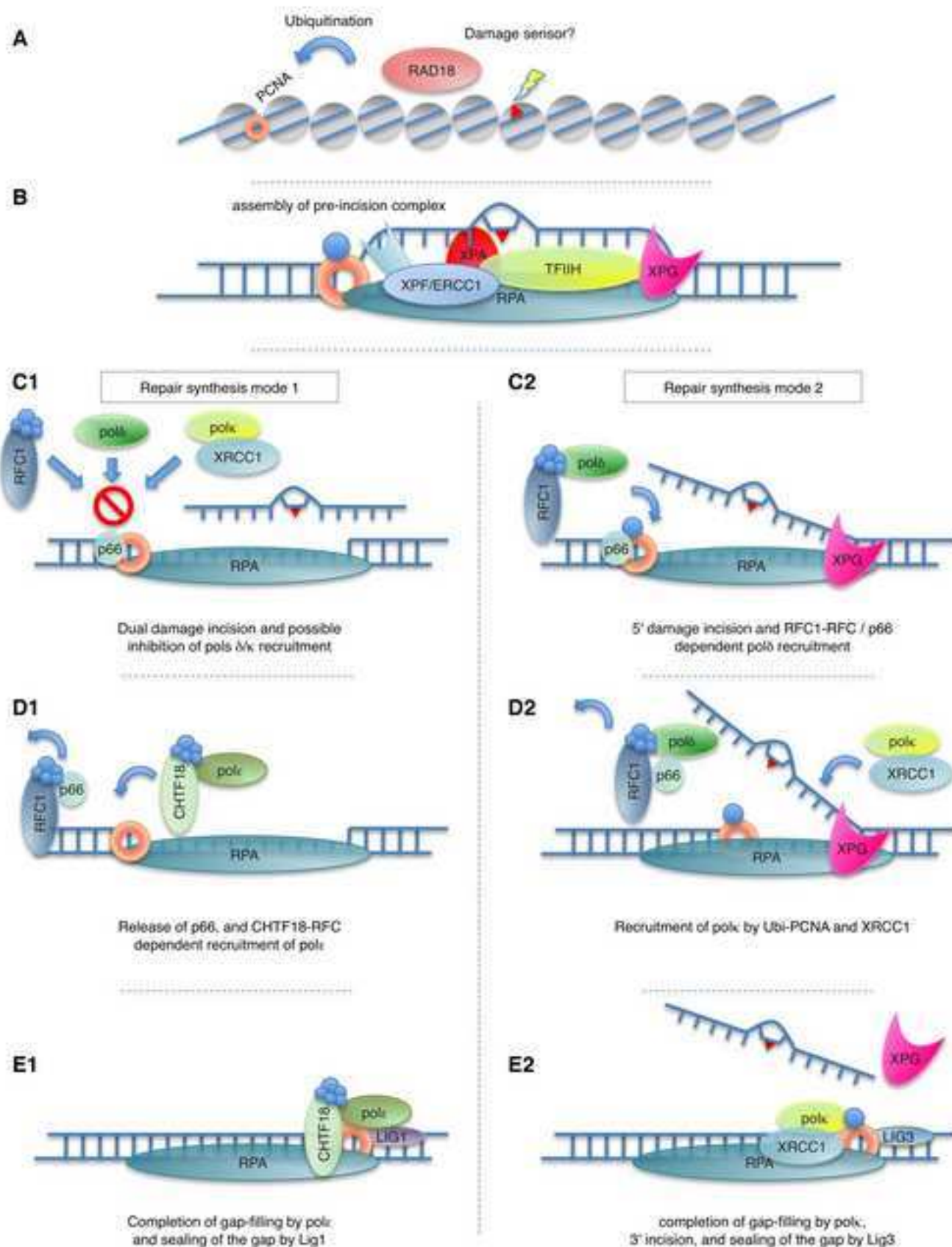


Figure 6

Supplementary Materials

Three DNA polymerases, recruited by different mechanisms, carry out NER repair synthesis in human cells.

Tomoo Ogi, Siripan Limsirichaikul, René Overmeer, Marcel Volker, Katsuya Takenaka, Ross Cloney, Yuka Nakazawa, Atsuko Niimi, Yoshio Miki, Nicolaas G Jaspers, Leon HF Mullenders, Shunichi Yamashita, Maria Fousteri and Alan R Lehmann

Experimental Procedures

Anti-polk antibodies

Two rabbits, SK04 and SK05, were immunised with an antigen that consisted of aa 603-870 of recombinant human polk protein, which was N-terminally-tagged with glutathione S-transferase (GST: the polk fragment was cloned into pGEX-P3 vector, expressed in *E.coli* strain BL21, followed by purification using Glutathione Sepharose HP; GE Healthcare Biosciences). Antisera were then affinity purified with the same polk fragment except that it was N-terminally-tagged with maltose binding protein (MBP: cloned into pMAL-X vector, purified by Amylose resin; New England Biolabs) rather

than GST. Purified IgG fractions from SK04 and SK05 were respectively termed K1 and K2.

Cell culture

The following cell lines were used for this study: MRC5V1, SV40 transformed normal human fibroblast; 48BR and VH25, normal human primary fibroblasts; XP21BR, primary fibroblast from XP-C patient; CS10LO, primary fibroblast from CS-B patient; XP15BR and XP25RO, primary fibroblasts from XP-A patient; XP20BE, primary fibroblast from XP-G patient. All cells were maintained in DMEM (WAKO) supplemented with 10% fetal calf serum (FCS, Hyclone) and antibiotics, unless otherwise noted.

For labeling with beads, trypsinised cells were cultured for 4 days in medium containing 0.5µm diameter latex-beads (PolyScience).

RNA interference

All the siRNA oligos used in the experiments were chemically modified *On-Target-plus*TM purchased from *Dharmacon* (the siRNA oligo sequences can be obtained from the authors upon request). *SmartPool*TM (a mixture of four different siRNA oligos designed for a single target gene in different regions) were used for all experiments unless otherwise noted. Individual siRNA oligos were also used for the experiments presented in Supplementary Figure S1 and S8. siRNA transfection was performed using HiPerfectTM (QIAGEN) transfection reagent according to the manufacturer's instruction. In typical experiments, 5nM of siRNA oligos were transfected in suspension, termed

'reverse transfection', followed by one additional transfection cycle 24 h after the first transfection (double transfection). Experiments were performed 48 h after the first siRNA transfection. Knockdown efficiencies were confirmed by western blot and immunofluorescence.

Local UV irradiation and immunofluorescence analysis

Experimental details have been described previously (Volker et al., 2001). 48BR primary cells were cultured in 5% FCS supplemented DMEM and maintained at confluent density during the time of experiments. Cells treated with siRNA and / or labeled with beads were grown on 15mm coverslips. The coverslips were washed with PBS followed by 40J/m² UVC (254nm) irradiation through a 5µm pore polycarbonate (PC) membrane filter (Millipore) unless otherwise noted. After incubation in the media and for the time period specified in the individual experiments, cells were triton-extracted with a buffer containing 0.2% Triton-X100, 300mM Sucrose in PBS for 30 sec, followed by fixation in 1% formaldehyde, 0.2% Triton-X100, and 300 mM sucrose in PBS for 20 min. The coverslips were blocked with PBS containing 10% FCS for 1h, subsequently incubated with the indicated primary antibodies diluted 1:200 in PBST (0.05% Tween 20) for 2 h, followed by extensive washing with PBST. For the coincident detection of polk and UV-photolesions, coverslips stained with the primary anti-polk antibody or a anti-XPB, S-19 antibody were fixed in 4% formaldehyde in PBS for 20 min, followed by denaturation of DNA in 5N HCl for 5min and extensive washing with PBST. The coverslips were then stained with anti-CPD, TDM2 antibody (1:2000 dilution in PBST). The coverslips stained with primary antibodies were then incubated for 1h with DAPI

(1ng /ml) and secondary antibodies conjugated with Alexa fluor 488 or 594 fluorescent dyes (Molecular Probes, 1:1000 dilution in PBST). After extensive washing, the coverslips were mounted with Aqua-poly-mount liquid (PolyScience). Photographs of the cells were captured with a Zeiss Axioobserver Z1 microscope equipped with CCD camera, and captured images were analysed with PhotoshopTM. Antibodies used for the immunofluorescent analyses were as follows: rabbit polyclonal anti-polk, K1 and K2 (this work); mouse monoclonal anti-RPA, RPA70-9 (Calbiochem); mouse monoclonal anti-XPB (p89), S-19 (Santa Cruz); mouse monoclonal anti-CPD, TDM2 (COSMO BIO); mouse monoclonal anti-Ki67, PP-67 (Abcam); mouse monoclonal anti-polδ (p125), A-9 (Santa Cruz); mouse monoclonal anti-polδ (p66), 2E3 (Abnova); mouse monoclonal anti-pole, 3A3.2 (Kind gift from Dr. Stuart Linn). **As shown in Table S1, the UV radiation treatment did not affect viability of the cells as determined by dye exclusion.**

Unscheduled DNA synthesis assay on coverslip by ethynyl deoxyuridine (EdU) incorporation

Experimental details have been described previously (Limsirichaikul et al., 2009). Briefly, normal 48BR or XPA deficient XP15BR primary fibroblasts were maintained at confluent density, transfected with indicated siRNAs (48BR only), followed by culturing on 15mm coverslips in DMEM supplemented with 5% FCS for 48h. The cells were washed once with PBS followed by mock treatment or global 10J/m² UVC irradiation. The cells were incubated for 2 h in DMEM supplemented with 0.1% FCS, and 10μM of 5-Ethynyl-2'-deoxyuridine (EdU). **Viability was unaffected by the UV treatment during the course of the experiment (Table S1).** After EdU incorporation, cells were extensively washed with PBS followed by fixation with 1% formaldehyde in PBS. The coverslips

were blocked for 1h with 10% FCS in PBS followed by 30 min incubation with 10mM CuSO₄ containing fluorescent dye coupling buffer (*Invitrogen*), containing Alexa Fluor 488 azide (Click-iT™, *Invitrogen*) and DAPI (1ng/ml). After extensive washing with PBS, coverslips were mounted with Aqua polymount. Photos were captured from at least five different fields from each coverslip and analysed with a KEYENCE BIOREVO BZ-9000 automated fluorescent microscope system. Averages and standard deviations of the fluorescent intensity differences between inside and outside of at least 250 nuclei were measured and calculated with ImageJ software.

Chromatin co-immunoprecipitation (ChIP) assay

Experimental details have been described previously (Fousteri et al., 2006). VH25, normal human primary fibroblast, and XP25RO, primary fibroblast from XP-A patient were grown to confluent density and cultivated for at least 7 days in 0.2% FCS supplemented DMEM to bring them into G0. Cells were then UVC irradiated (20J/m²), and incubated at 37°C for 1 h prior to *in vivo* crosslinking and ChIP. *In vivo* crosslinking, lysis of the cells, chromatin purification and immunoprecipitation, and reversal of the crosslinks prior to western blotting were described previously (Moser et al., 2007). Antibodies used for the immunoprecipitation and western blotting were as follows: mouse monoclonal anti-PCNA, PC-10 (Abcam); mouse monoclonal anti-XRCC1, 3-3-25 (Abcam); mouse monoclonal anti-RPA70, RPA70-9 (Calbiochem); rabbit polyclonal anti-polk, K1 (this work); mouse monoclonal anti-polδ (p125), A-9 (Santa Cruz); mouse monoclonal anti-polε, 93H3A (Abcam); mouse monoclonal anti-LigIII, 1F3 (GenTex), rabbit polyclonal anti-polη, ab17725 (Abcam).

Detection of ubiquitinated PCNA in quiescent XP-deficient cells

Normal (48BR) and XP (XPA, XP15BR; XPC, XP21BR) primary fibroblasts were used. Confluent cells were cultured in 0.2% FCS supplemented DMEM for 5 days to bring them to quiescence (G0). Cell populations in G0 as well as cycling cells were determined by immunostaining the cells with the cell cycle marker, anti-ki67 mouse monoclonal antibody (PP-67), and the EdU incorporation assay (described above), respectively. Ki-67 positive (cycling), or EdU positive (S-phase) cells in the populations used were as follows: 48BR, Ki-67 positive 9/652 (1.4%), EdU positive 0/652 (<0.15%); XPA, Ki-67 positive 20/707 (2.8%), EdU positive 2/707(0.3%); XPC, Ki-67 positive 1/766 (0.1%), EdU positive 0/766 (<0.13%). Cells were globally (20J/m²) UVC irradiated or 10mM hydroxyurea treated, followed by incubation for the indicated period in serum depleted medium. As a control, MRC5V1 cells were globally irradiated (20J/m² UVC) or 10mM hydroxyurea treated and incubated for 4h. Cells were then washed with PBS and harvested. For the detection of chromatin-bound PCNA, cells were treated with ice cold 0.2% Triton-X100, 300mM Sucrose in PBS for 10 min, followed by washing with the same buffer before harvesting. Total cell lysates were resolved by 8% SDS-PAGE followed by transfer to a PVDF membrane. PCNA and Ubiquitinated PCNA were detected by mouse monoclonal anti-PCNA antibody (PC10).

Supplementary Table S1. Cell viabilities after UV irradiation.

	48BR		XP15BR		XP21BR	
Time after UV irradiation	2h	6h	2h	6h	2h	6h
0J/m ²	97±1.7	NA	97±1.5	NA	98±1.0	NA
10J/m ² global	97±0.6	97±1.3	94±4.3	92±3.1	95±4.6	93±3.0
20J/m ² global	98±1.9	96±2.0	94±2.7	84±5.5	95±3.1	86±6.1
40J/m ² local (5µm)	97±2.2	96±1.8	96±2.4	96±2.6	98±1.0	97±1.8

Cell viabilities for the conditions we used were determined by trypan blue dye exclusion assay as follows: 48BR, XP15BR, and XP21BR cells were plated on 3cm diameter dishes as well as coverslips, and UVC irradiated globally at 10J/m² and 20J/m² (dish), or locally with 40J/m² through a 5µm pore PC filter (coverslips), or mock treated. After UV irradiation, the cells were cultured for 2h or 6h in DMEM supplemented with 10% FCS. The dishes and coverslips were washed with PBS, and stained with 0.08% trypan blue in PBS for 10min at room temperature.

Supplementary Figure S1 Anti-polk antibodies

(A and B) Western-blot analyses of polk expression. Rabbit polyclonal anti-human-polk antibodies, K1 (A), and K2 (B), detect endogenous polk in human fibroblasts. 157, mouse *Polk* K/O embryonic fibroblasts expressing GFP-tagged human *POLK* cDNA (Ogi et al., 2005); MRC5V1 cells were transfected with *Dharmacon On-target-plusTM* siRNA oligos (4 individual oligos 05-08, or *SmartPoolTM*, which is a mixture of 4 oligos) against human *POLK* (*siPOLK*) and scrambled *SmartPoolTM* non-targeting control (*siNTC*). Asterisks indicate non-specific band.

Supplementary Figure S2 Accumulation of polk at sites of DNA damage (ALD)

(A) Colocalisation of UV photolesions and polk. 48BR primary cells were locally UVC-irradiated ($5\mu\text{m}$, 40 J/m^2), followed by 1h incubation without inhibitors. Coverslips were immunostained with rabbit anti-XPB, S-19 (top), or rabbit anti-polk, K-1 (bottom) antibodies (red), followed by DNA denaturation and detection of photolesions with mouse anti-CPD, TDM2 antibody (green). (B) 48BR primary cells treated with non-targeting control siRNA and cultured with blue latex beads were co-cultured with no-beads-labeled cells treated with *siPOLK*. KD, *POLK* knockdown with *siPOLK*; Ctr, no-knockdown with *siNTC*, locally UVC-irradiated (40 J/m^2), incubated for 30min with media supplemented with 10mM hydroxyurea; cells were then immunostained with mouse anti-RPA70 (RPA70-9, green), and rabbit anti-polk (K1, red). Note the red and green staining in the cells labelled with blue beads (Ctr) but only green staining in the cells not labelled with blue beads (KD), confirming that the red spots do indeed represent polk. (C-F) Cell cycle dependent ALD of polk and enhanced ALD of polymerases by

replication inhibitor treatment. (C) 48BR cells were cultured in low-serum (0.5%) medium for 4 days, locally UVC irradiated (40 J/m²) followed by 1h incubation with low-serum medium (without HU) and immunostaining with anti-polk (K1, red) and mouse anti-Ki67 (PP-67, green) antibody. Cyc, Ki67 positive cycling cells; G0, Ki67 negative noncycling G0 cells. (D) Locally UV irradiated 48BR cells were cultured for 30 min in complete medium with 10mM HU. Increased staining of RPA70 (green) distinguishes S-phase cells, polk (red). Circles indicate damage dependent local spots. (E, F) 48BR cells were maintained at confluent density and locally UVC irradiated (40J/m² through 5um pore PC filter), followed by incubation for 30min in media supplemented without (E) or with replication inhibitors, 10mM hydroxyurea (F). K1 anti-polk (red) and mouse A-9 anti-polδ p125 (green) antibodies were used for the immunostaining. (G-J) **Polk ALD in normal and XP-deficient human fibroblasts.** (G) XP21BR XP-C cells, (H) XP20BE XP-G cells, (I) 48BR primary cells in which XPF had been depleted with siRNA and (J) CS10LO CS-B cells were cocultured with normal 48BR cells containing blue beads (except for I). Cells were locally UVC-irradiated (40 J/m²), incubated for 1h without inhibitors; cells were then immunostained with mouse anti-RPA70 (RPA70-9, green), and rabbit anti-polk (K1, red). Note the colocalisation of RPA and polk spots in all nuclei in (J) but only in the normal cells in (G) and (H), and no polk ALD in (I). (K) **FACS analysis of cells transfected with GFP-POLK constructs.** MRC5VI cells were transfected with constructs containing wild-type or the indicated mutants of GFP-POLK. After two days, the cells were analysed by flow cytometry (BD FACSaria). GFP fluorescence intensity distribution profiles and average fluorescence intensity are shown. Av, average FITC-Area values.

Supplementary Figure S3 **Unscheduled DNA synthesis (UDS) measured by Ethynyl dU (EdU) incorporation**

(A, B) UDS measured by Ethynyl dU (EdU) incorporation. 48BR primary cells (cultured at sub-confluent density) were mock treated **(A)** or globally UVC irradiated (10J/m^2) **(B)**, followed by 2h incubation in serum depleted medium supplemented with $10\mu\text{M}$ EdU. Incorporated EdU was detected after AlexaFluor488 azide conjugation (green); Phase-contrast (gray). **(C) Depletion of polk, pol δ or RAD18 results in decreased UDS.** 48BR cells were transfected with indicated siRNAs, globally UVC-irradiated (10 J/m^2) followed by EdU incorporation for 2h. Cells were fixed and stained as described above. DAPI (left, blue); EdU (right, green). **(D) Effect of differently designed siRNAs on UDS.** 48BR cells were treated with *SmartPool*TM (a mixture of four different siRNA oligos designed for a single target gene in different regions) non-targeting control (*siNTC*), *XPA* targeting *SmartPool*TM (*siXPA*), *POLK* targeting *SmartPool*TM (*siPOLK-Sm*, closed-box), which consists of four individual *POLK* targeting oligos (*siPOLK 05-08*, open-box), and *RAD18* targeting *SmartPool*TM (*siRAD18-Sm*, closed-box), which consists of four individual *RAD18* targeting oligos (*siRAD18 05-08*, open-box). UDS was measured using the EdU assay above described (10J/m^2 global UVC, 2h). Bars and error bars respectively indicate averages and standard deviations of nuclear fluorescent intensity measured in at least 250 nuclei from at least 5 different positions.

Supplementary Figure S4 **ALD of pole**

48BR primary cells were locally UVC-irradiated ($5\mu\text{m}$, $40\text{J}/\text{m}^2$), followed by 1h incubation. (A) Cells were pre-fixed with 4% formaldehyde in PBS for 10min, followed by permeabilisation with 0.5% Triton X100 in PBS for 5min, or (B) extracted with 0.2% Triton-X100, 300mM Sucrose in PBS for 30 sec, followed by fixation in 1% formaldehyde, 0.2% Triton-X100, and 300 mM sucrose in PBS for 20 min. Cells were then immunostained with mouse anti-pole (3A3.2, green), and rabbit anti-XPB (S-19, red) antibodies. Note that pole is extracted under standard immunostaining conditions.

Supplementary References

Fousteri, M., Vermeulen, W., van Zeeland, A.A., and Mullenders, L.H. (2006). Cockayne syndrome A and B proteins differentially regulate recruitment of chromatin remodeling and repair factors to stalled RNA polymerase II in vivo. *Mol Cell* 23, 471-482.

Limsirichaikul, S., Niimi, A., Fawcett, H., Lehmann, A., Yamashita, S., and Ogi, T. (2009). A rapid non-radioactive technique for measurement of repair synthesis in primary human fibroblasts by incorporation of ethynyl deoxyuridine (EdU). *Nucleic Acids Res* 37, e31.

Moser, J., Kool, H., Giakzidis, I., Caldecott, K., Mullenders, L.H., and Fousteri, M.I. (2007). Sealing of chromosomal DNA nicks during nucleotide excision repair requires XRCC1 and DNA ligase III alpha in a cell-cycle-specific manner. *Mol Cell* 27, 311-323.

Ogi, T., Kannouche, P., and Lehmann, A.R. (2005). Localisation of human Y-family DNA polymerase kappa: relationship to PCNA foci. *J Cell Sci* 118, 129-136.

Volker, M., Mone, M.J., Karmakar, P., van Hoffen, A., Schul, W., Vermeulen, W.,
Hoeijmakers, J.H., van Driel, R., van Zeeland, A.A., and Mullenders, L.H. (2001).
Sequential assembly of the nucleotide excision repair factors in vivo. *Mol Cell* 8, 213-
224.

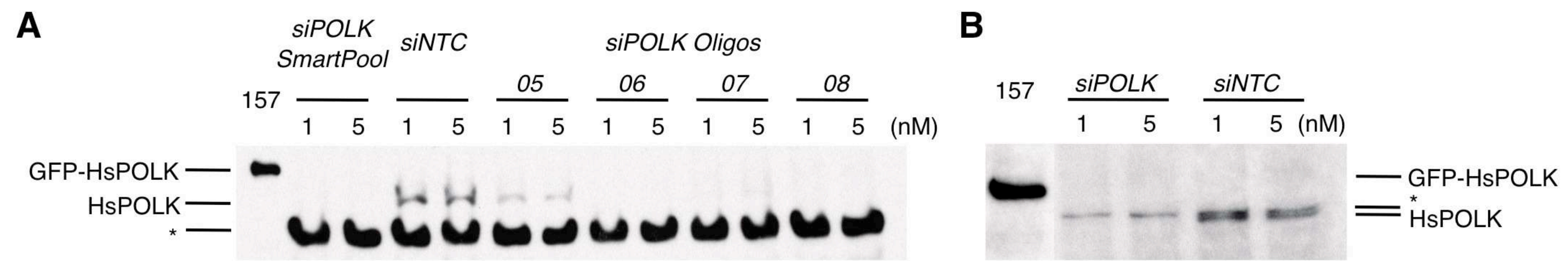


Figure S1

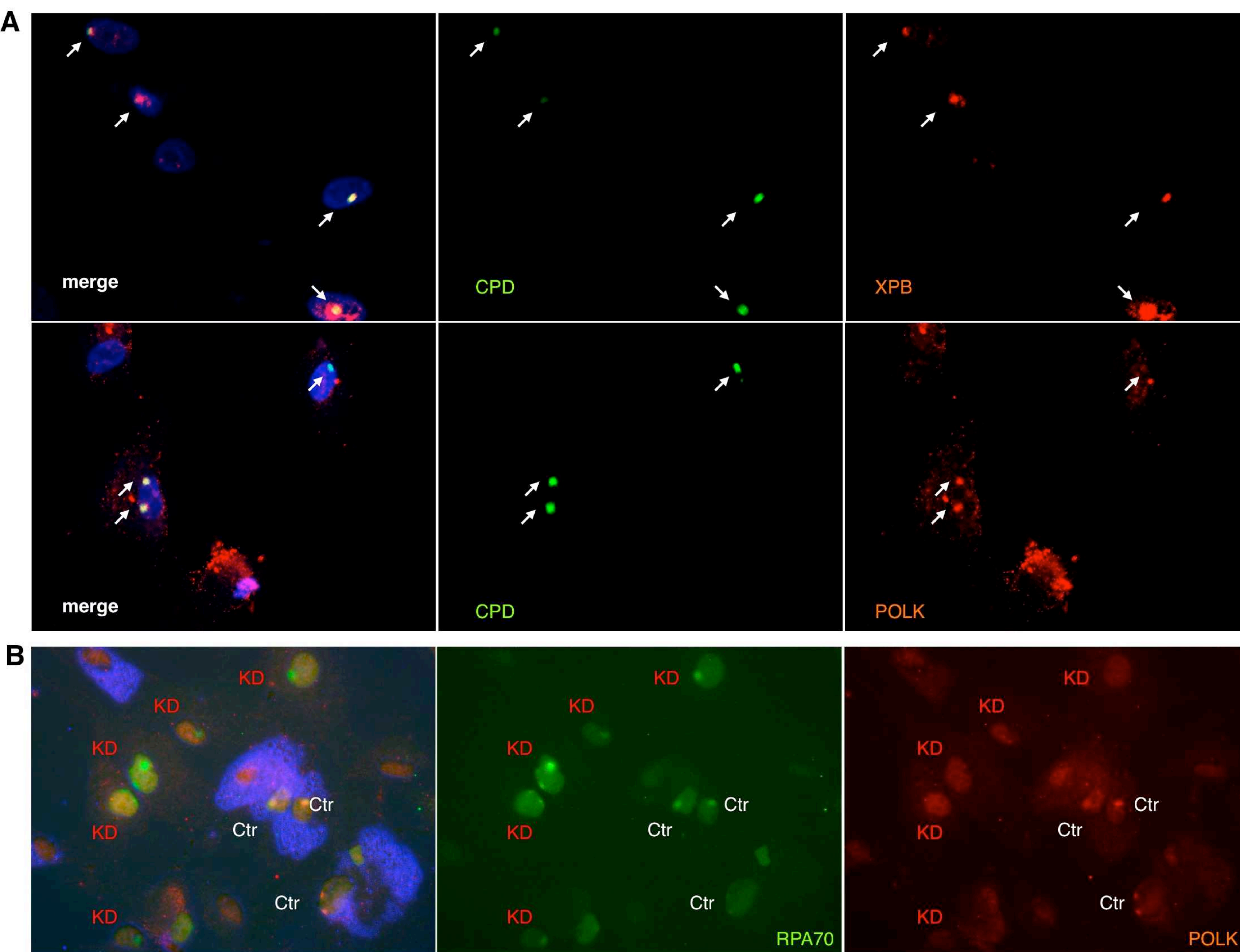


Figure S2

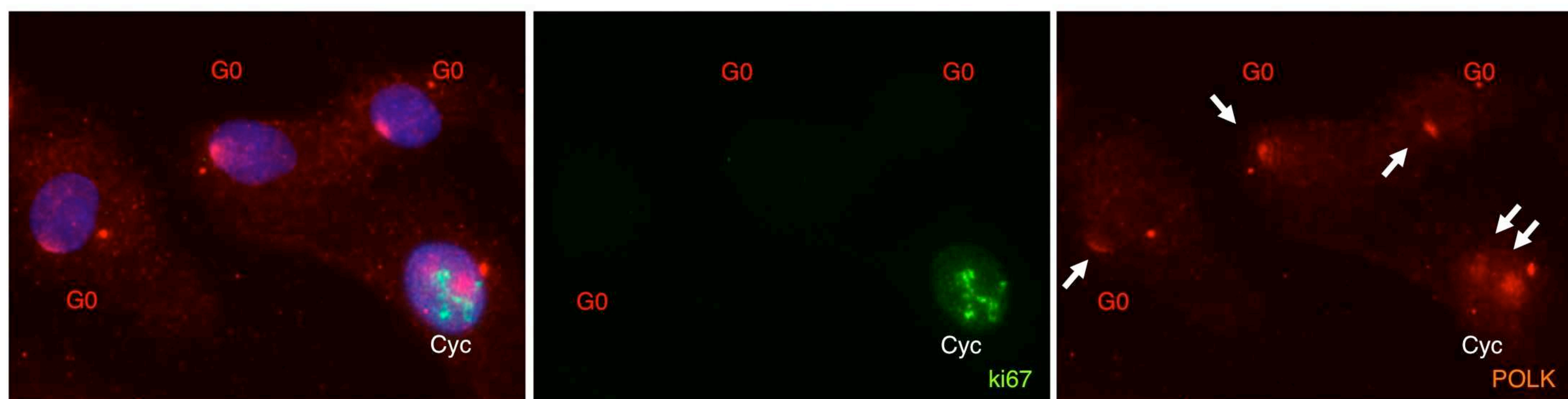
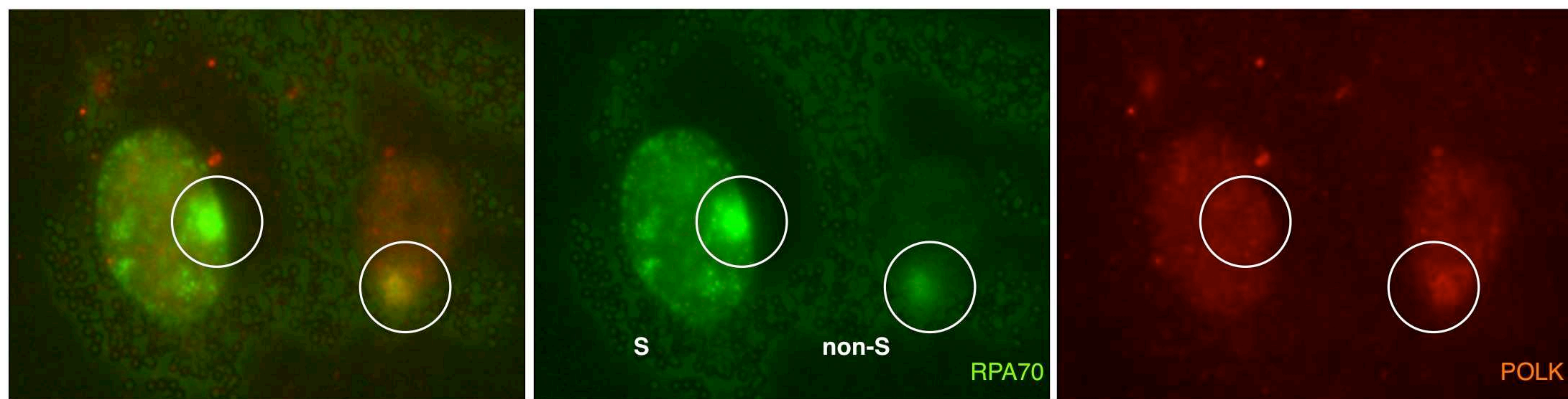
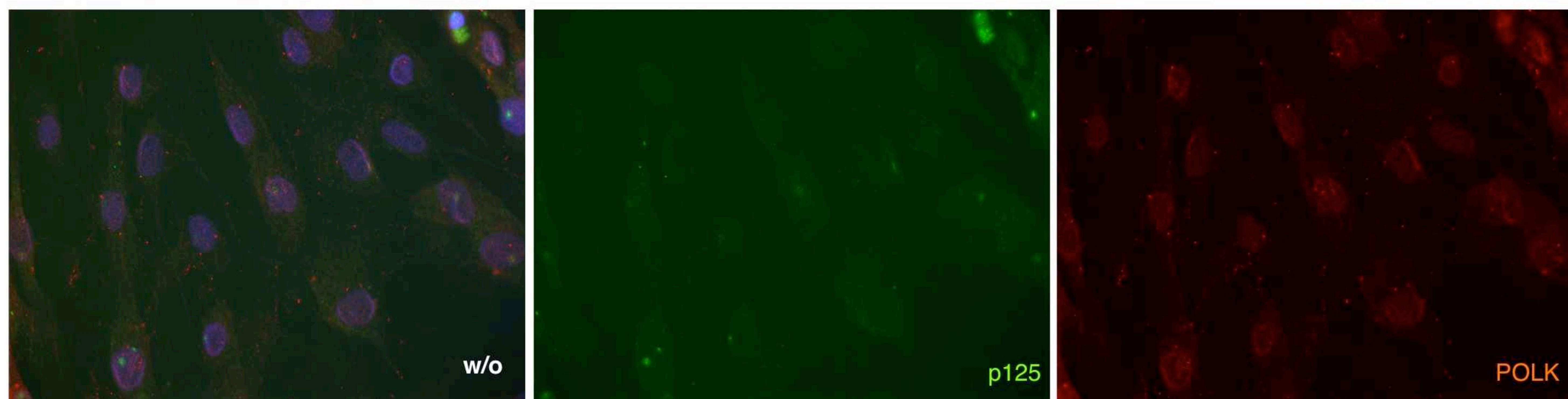
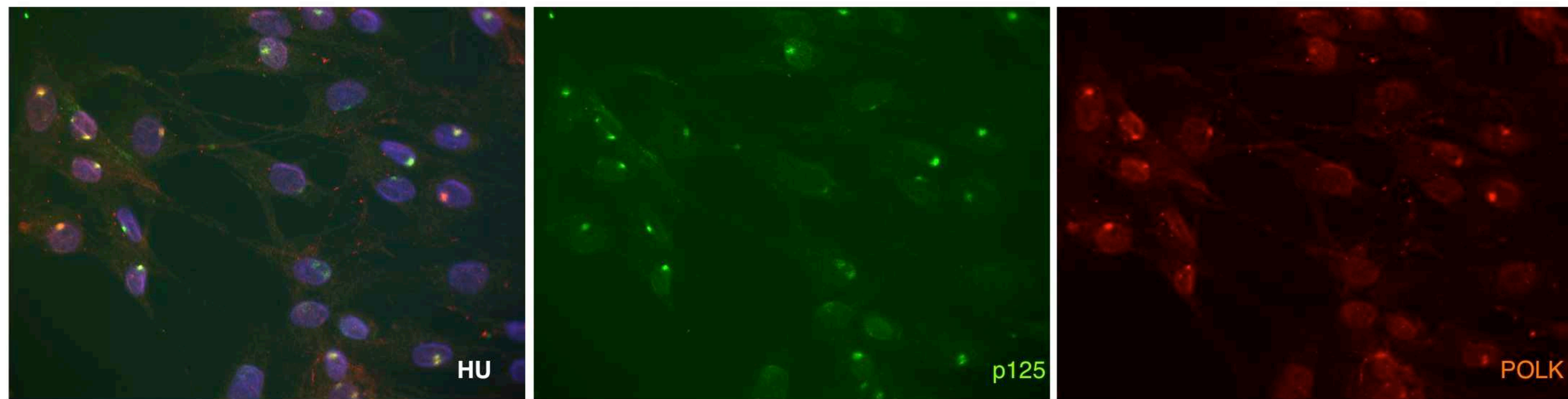
C**D****E****F**

Figure S2 - continued

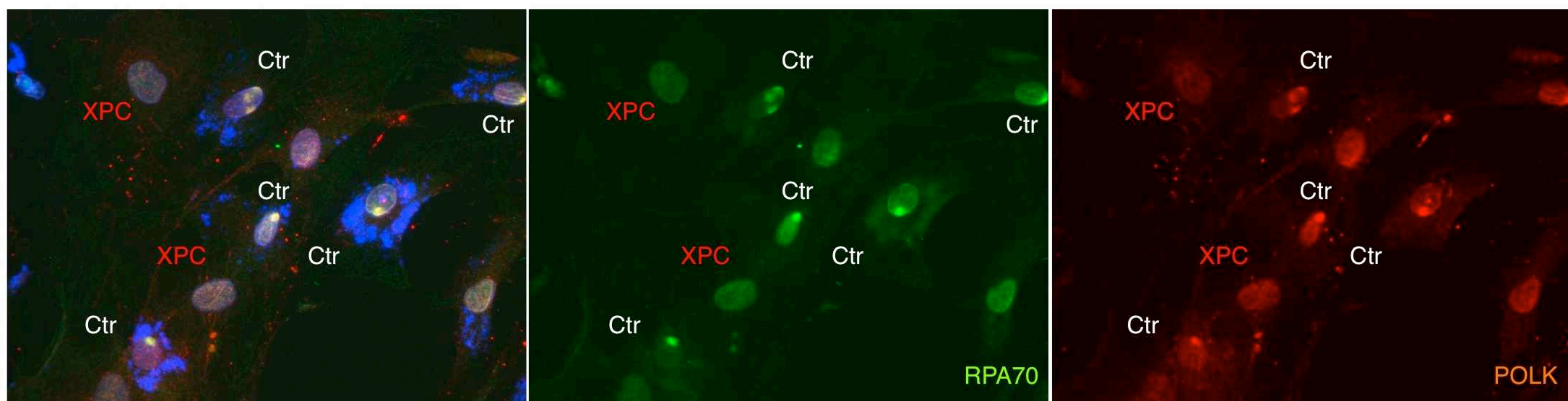
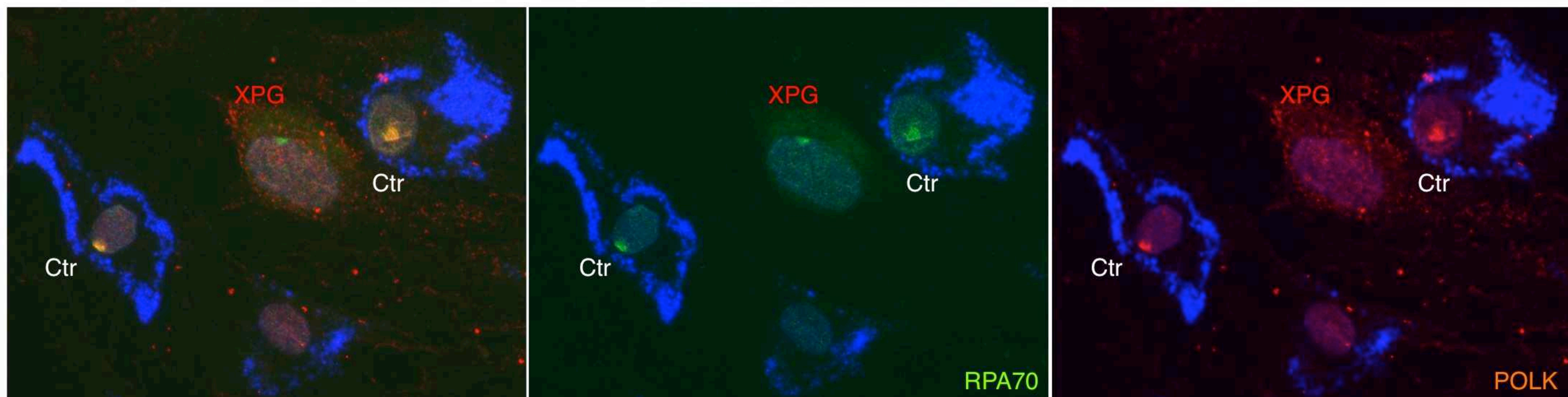
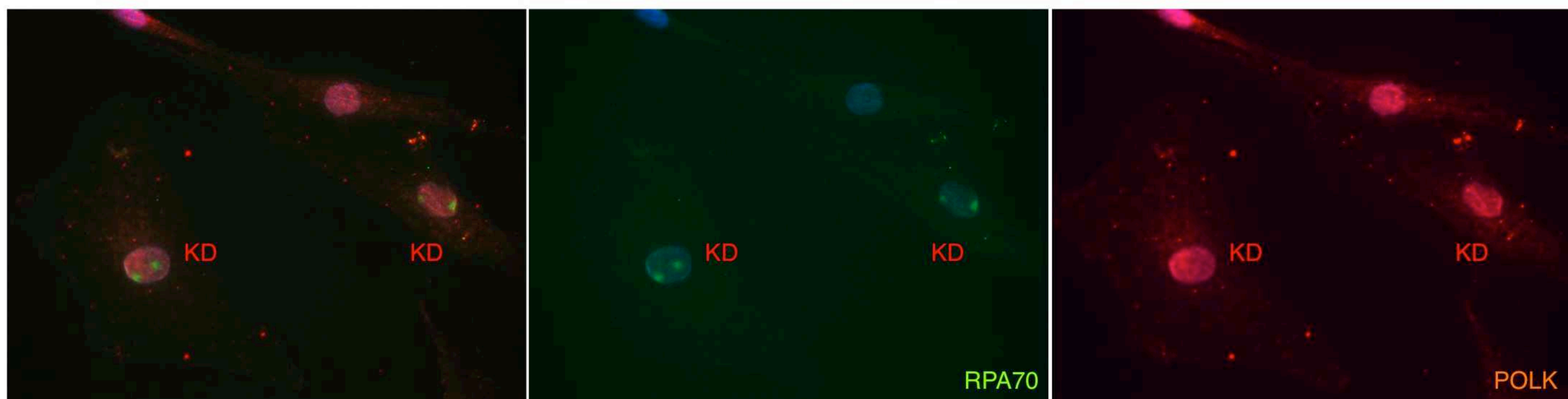
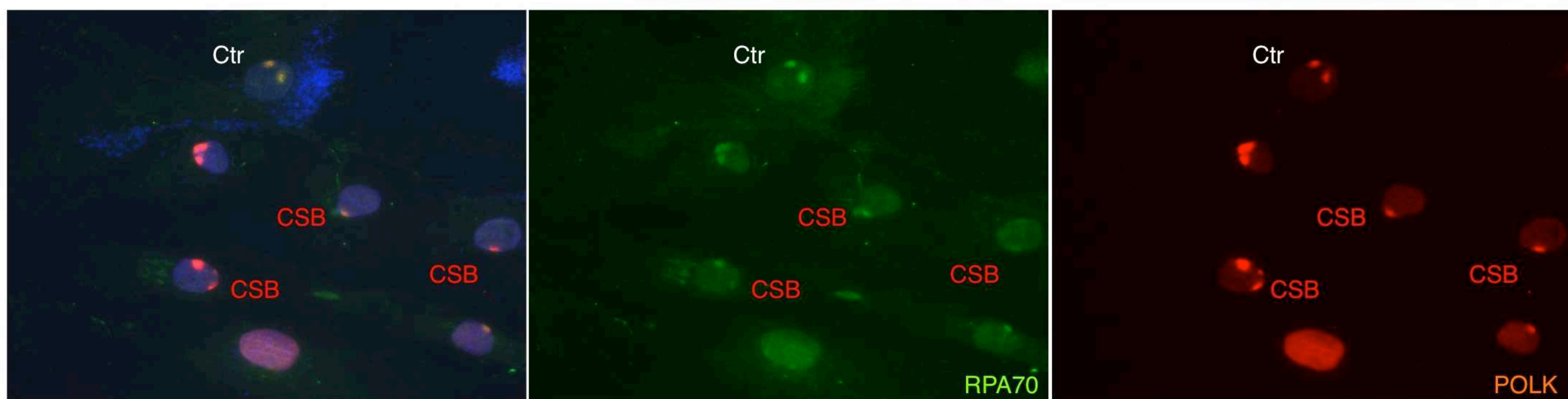
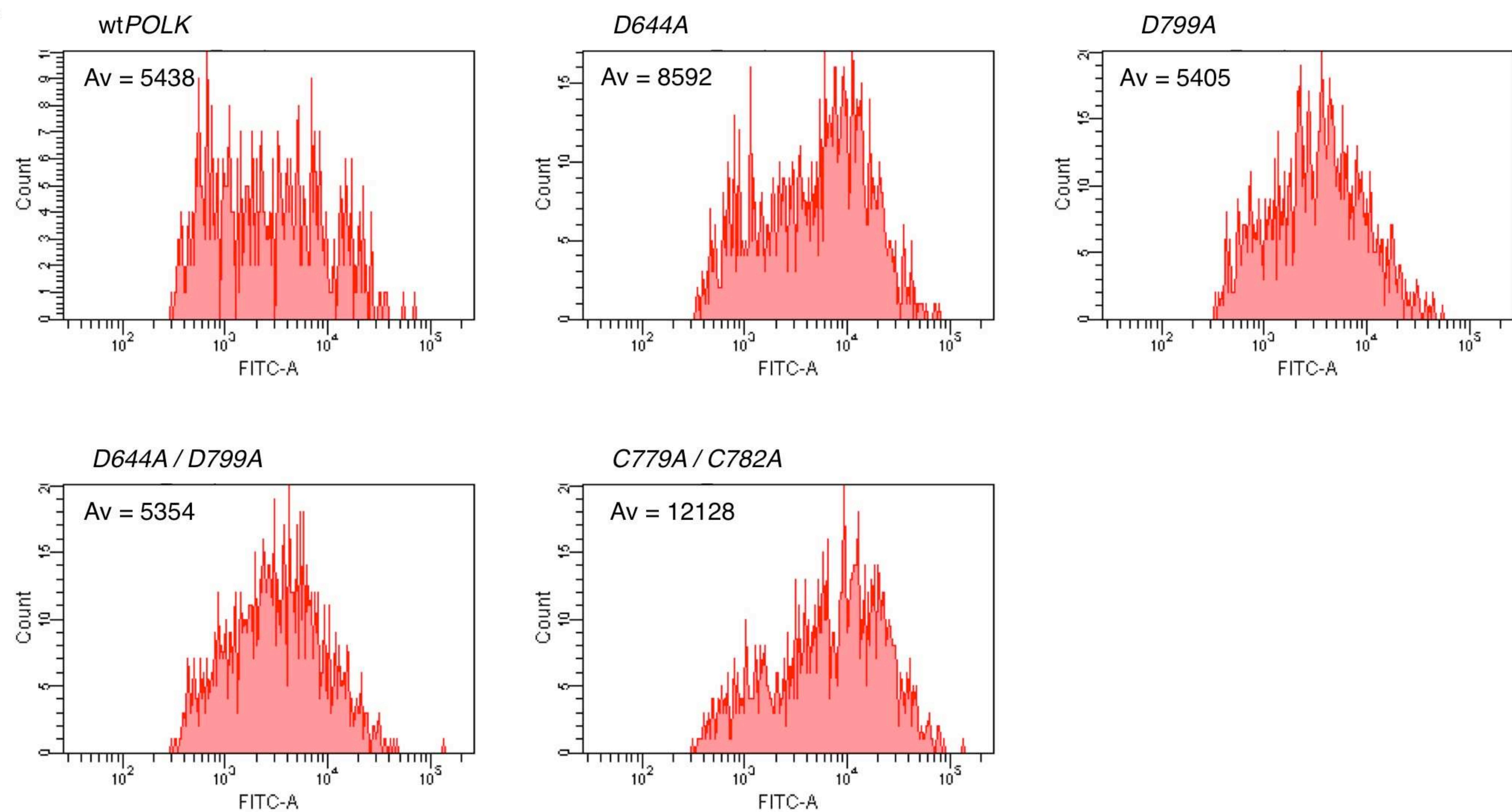
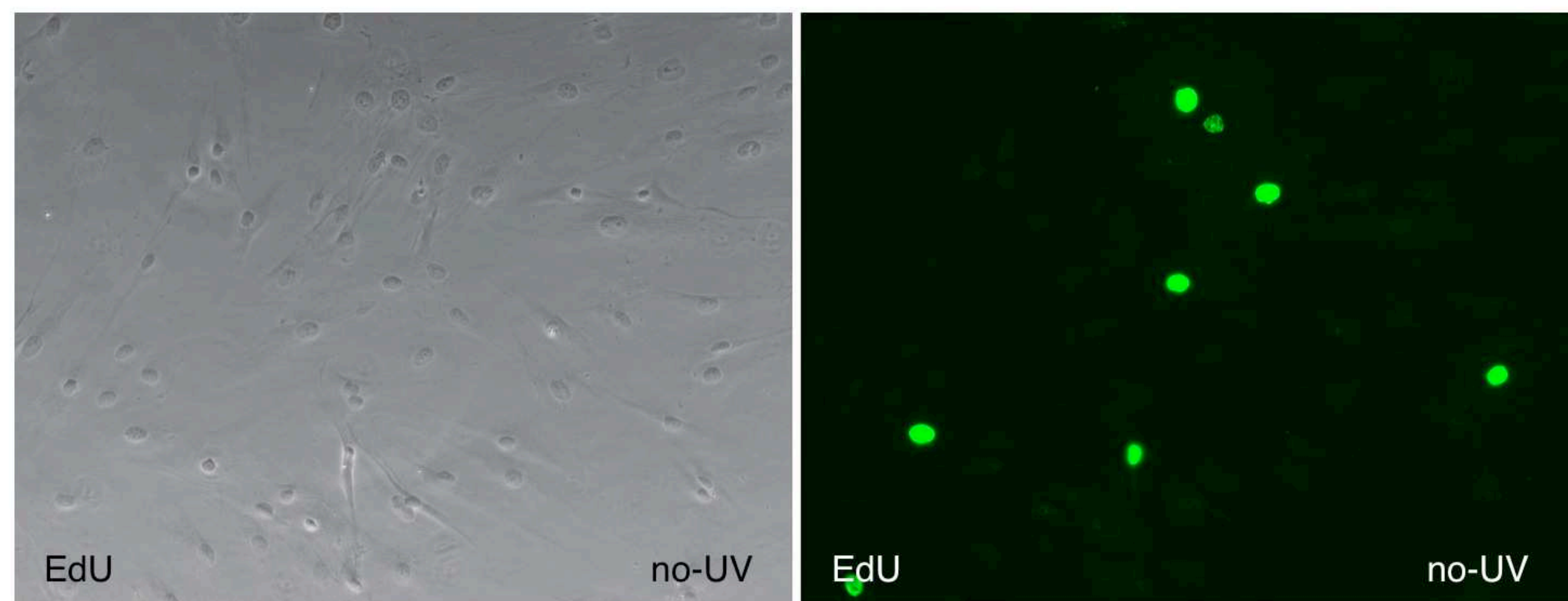
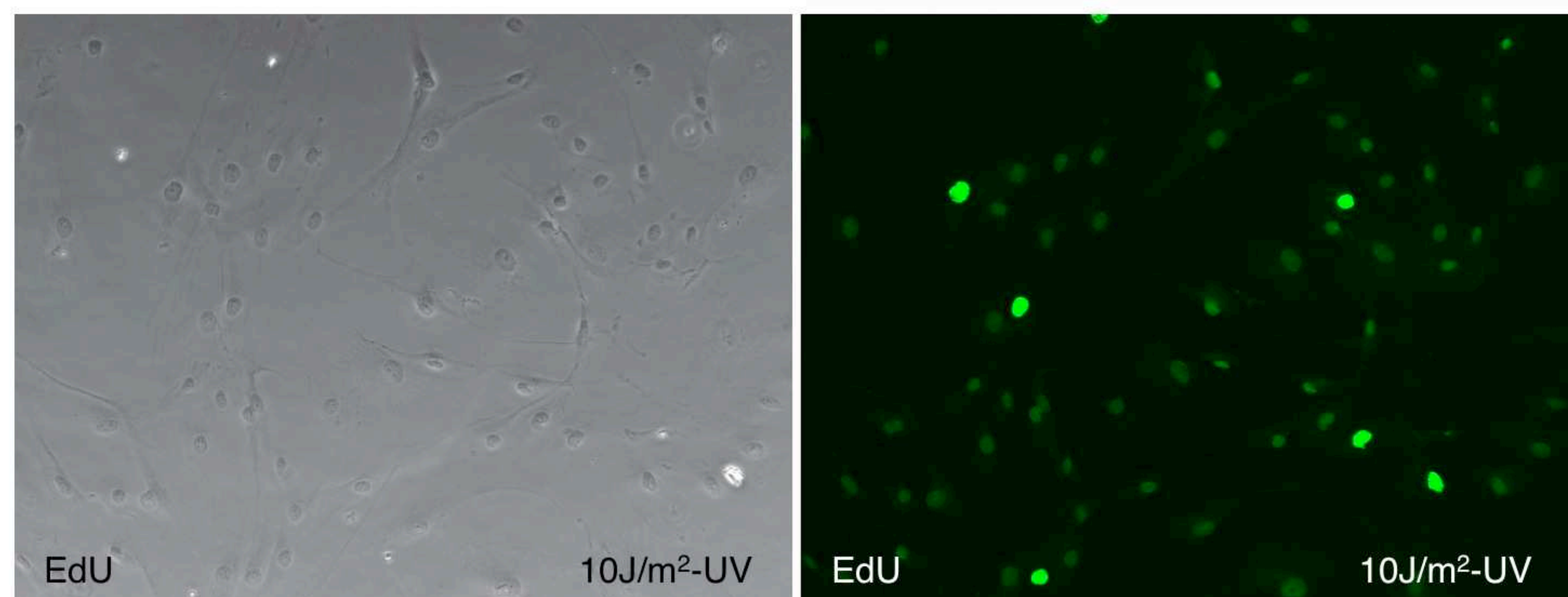
G**H****I****J**

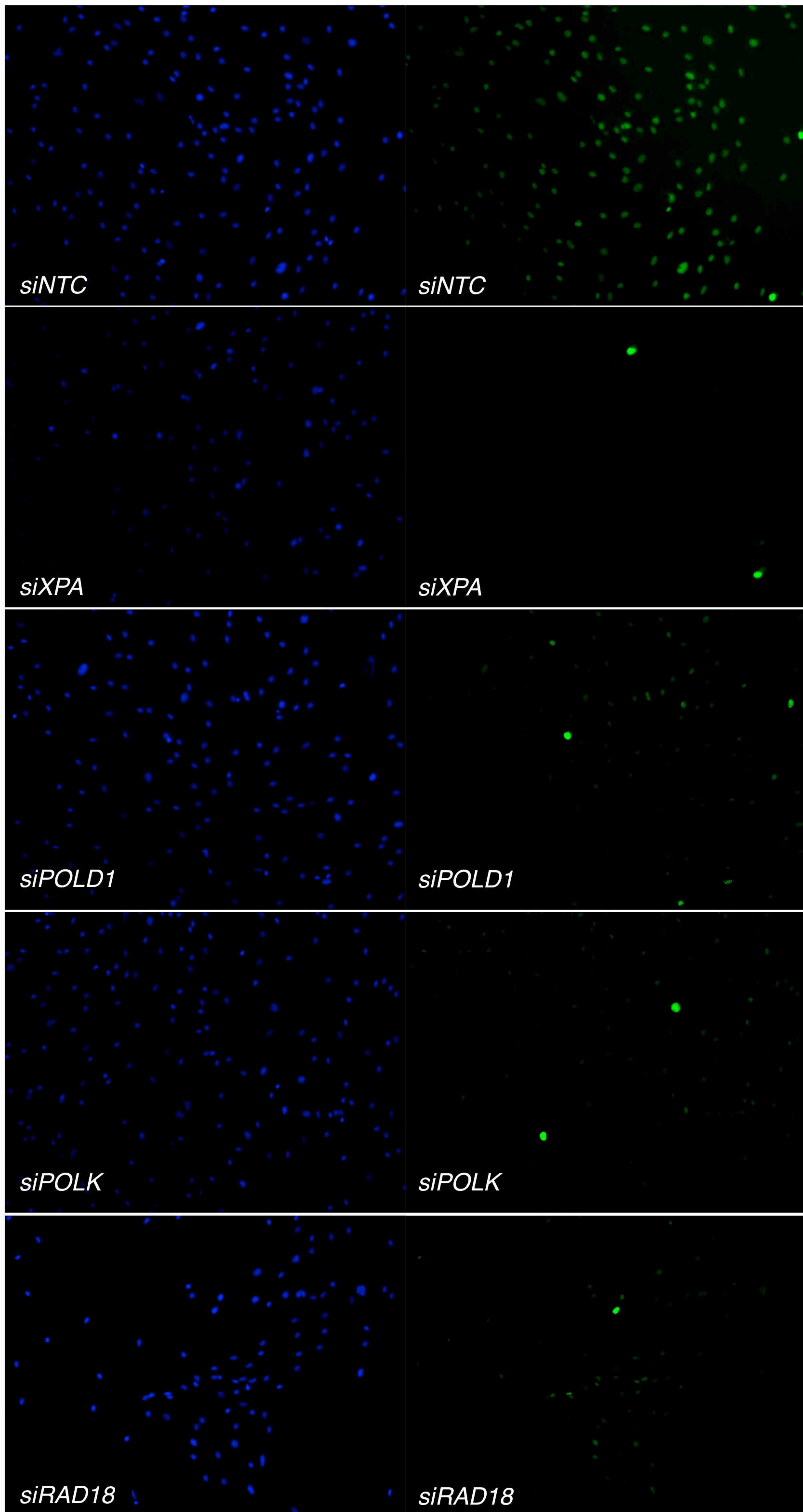
Figure S2 - continued

K**Figure S2 - continued****A****B****Figure S3**

C

DAPI

EdU

**Figure S3 -
continued**

D

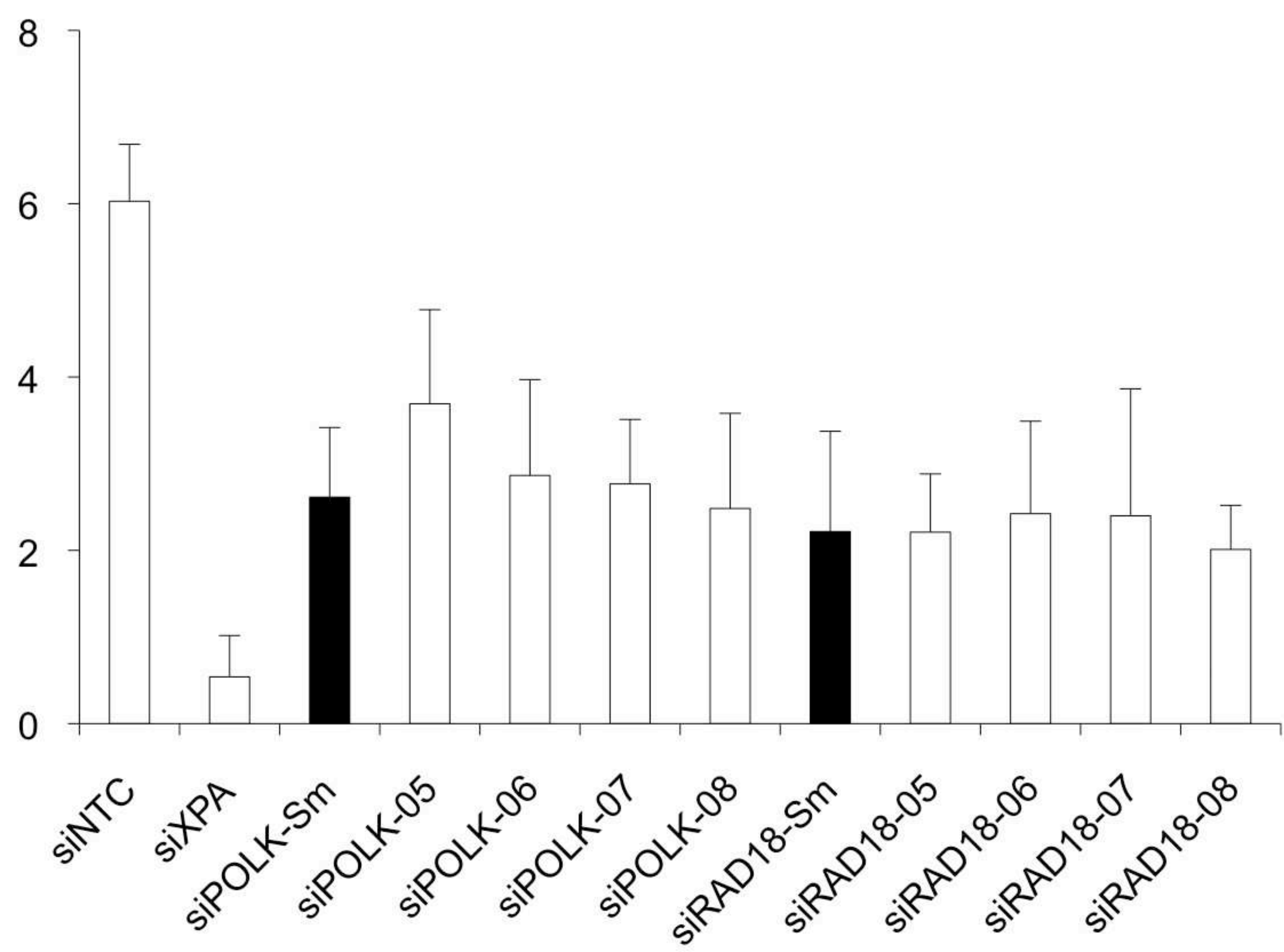
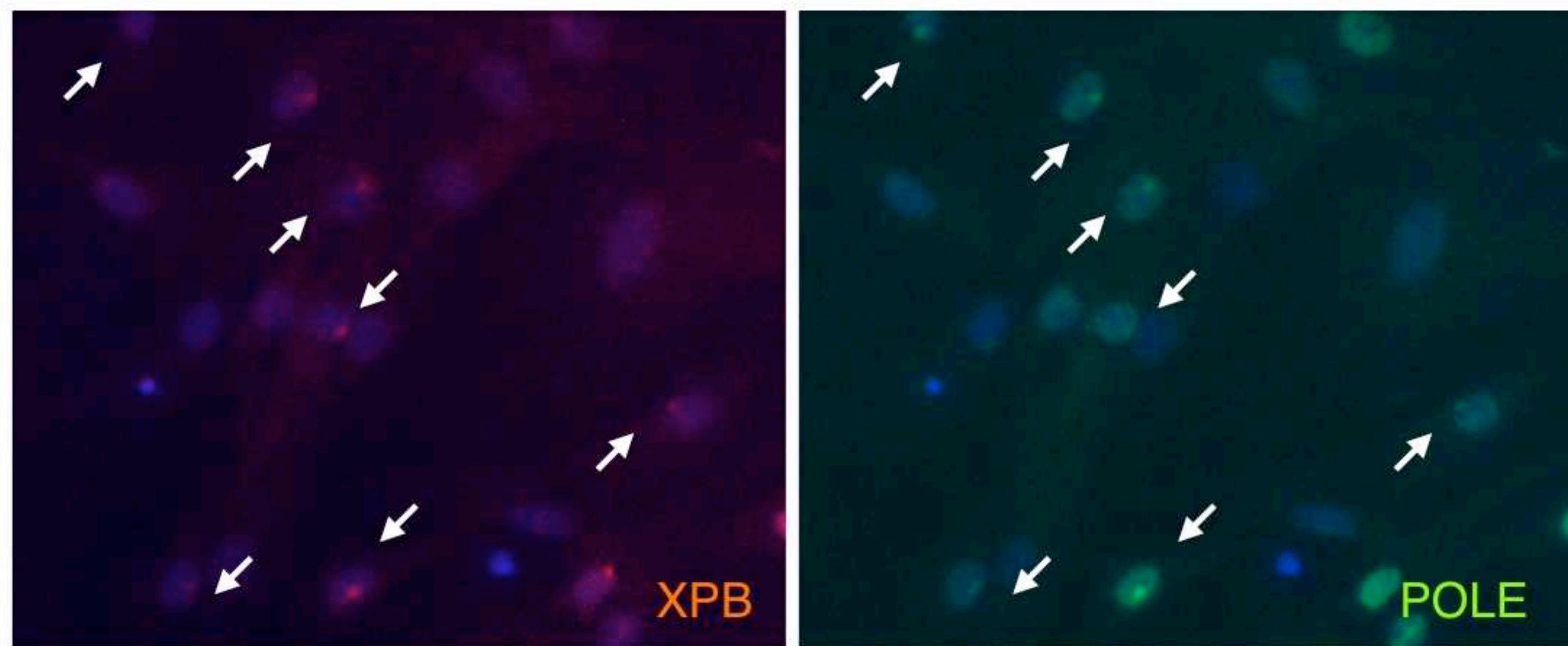


Figure S3 - continued

A



B

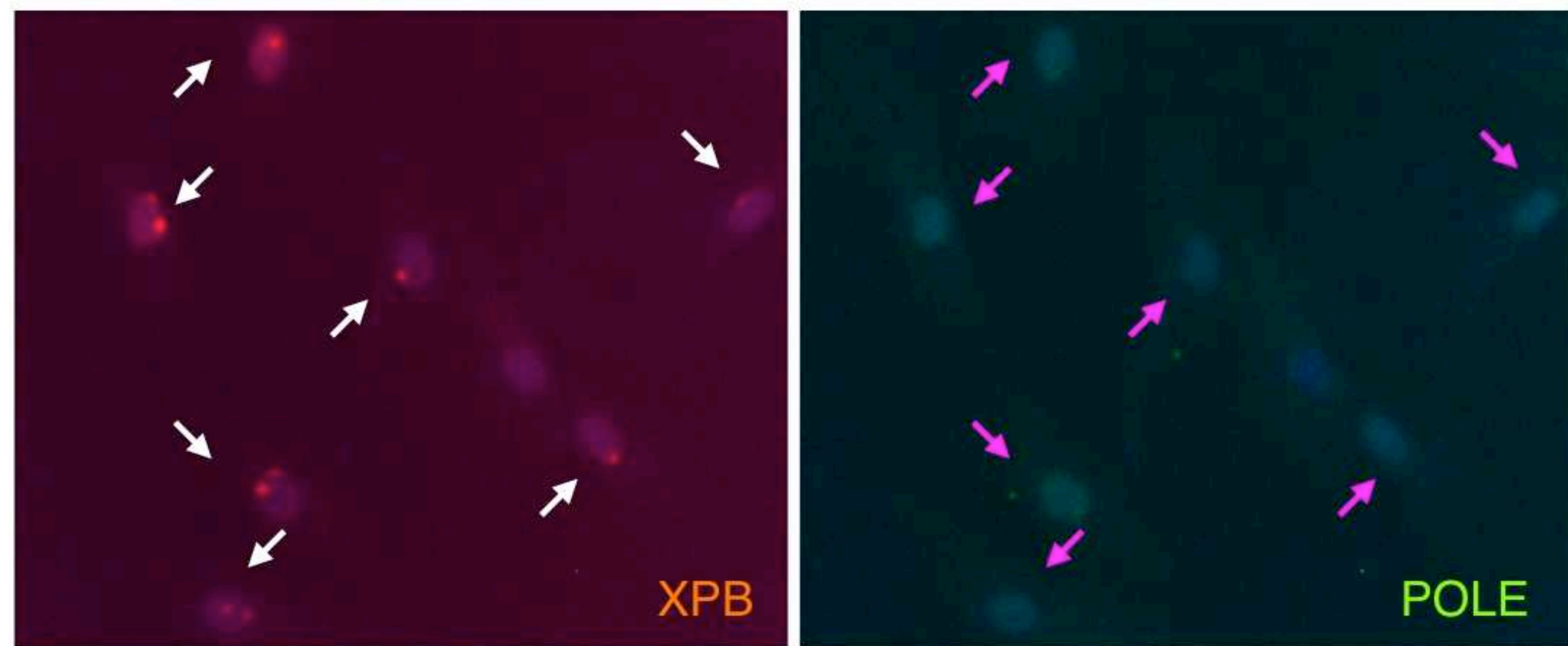


Figure S4